KU LEUVEN

FACULTEIT INGENIEURSWETENSCHAPPEN

Biomechanical evaluation of a patient-specific TMJ prosthesis using FEM

David Pastor Alonso

Thesis submitted to
obtain the degree of Master
of Science in Biomedical Engineering

Promoters:
Prof. Dr. Ir. Jos Vander Sloten
Prof. Dr. mult. Maurice Mommaerts

Academic Year 2018 - 2019

Master of Science in Biomedical Engineering

KU LEUVEN

FACULTEIT INGENIEURSWETENSCHAPPEN

Biomechanical evaluation of a patient-specific TMJ prosthesis using FEM

David Pastor Alonso

Thesis submitted to
obtain the degree of Master
of Science in Biomedical Engineering

Promoters:
Prof. Dr. Ir. Jos Vander Sloten
Prof. Dr. mult. Maurice Mommaerts

Assessor:
Prof. Dr. Ir. Harry Van Lenthe
Prof. Dr. Ir. Nele Famaey

Mentors:
Ir. Stijn Huys

Academic Year 2018 - 2019

© Copyright by KU Leuven

Zonder voorafgaande schriftelijke toestemming van zowel de promoter(en) als de auteur(s) is overnemen, kopiëren, gebruiken of realiseren van deze uitgave of gedeelten ervan verboden. Voor aanvragen tot of informatie i.v.m. het overnemen en/of gebruik en/of realisatie van gedeelten uit deze publicatie, wend u tot de KU Leuven, Faculteit Ingenieurswetenschappen - Kasteelpark Arenberg 1, B-3001 Heverlee (België). Telefoon +32-16-32 13 50 & Fax. +32-16-32 19 88.

Voorafgaande schriftelijke toestemming van de promoter(en) is eveneens vereist voor het aanwenden van de in dit afstudeerwerk beschreven (originele) methoden, producten, schakelingen en programma's voor industrieel of commercieel nut en voor de inzending van deze publicatie ter deelname aan wetenschappelijke prijzen of wedstrijden.

© Copyright by KU Leuven

Without written permission of the supervisor(s) and the authors it is forbidden to reproduce or adapt in any form or by any means any part of this publication. Requests for obtaining the right to reproduce or utilize parts of this publication should be addressed to KU Leuven, Faculty of Engineering Science - Kasteelpark Arenberg 1, B-3001 Heverlee (Belgium). Telephone +32-16-32 13 50 & Fax. +32-16-32 19 88.

A written permission of the supervisor(s) is also required to use the methods, products, schematics and programs described in this work for industrial or commercial use, and for submitting this publication in scientific contests.

Foreword

The development of this thesis has been made possible by the efforts of many people to whom I would like to express my most sincere appreciation:

To my parents since they have made every single moment of my studies possible. For their constant encouragement and willingness to support me and push me towards my dreams.

To my supervisor Ir. Stijn Huys who advised me and provided me with the necessary information and material to make this a successful thesis, and who was always ready to invest his time in the interest of this project.

To my promoters Professor Jos Vander Sloten and Professor Mommaerts for pushing me to critically think about this field of work and guide me at all moments in the right direction.

To my assessors Professor Nele Famaey and Professor Harry Van Lenthe whose help was essential and who are always predisposed to lend a hand to who needs it.

To the KU Leuven institution and professors of the Master in Biomedical Engineering for providing the optimal learning environment.

David Pastor Alonso

Table of Contents

Foreword iii
Table of Contents v
Abstract ix
List of figures and tables xi
List of figures xi
List of tables xiii
List of abbreviations and symbols xiv
Chapter 1 - Introduction 1
1.1- Problem statement 1
1.2- Objectives 2
1.3- Chapters Overview 3
Chapter 2 - Literature review 4
2.1- Introduction 4
2.2- The Temporomandibular Joint 4
2.2.1- The articular disc 4
2.2.2- Ligaments 5
2.2.3- Movements 6
2.2.4- TMJ replacement 7
2.3. The Finite Element Model 8
2.3.1- TMJ TJR research 8
2.3.2- Static and dynamic simulations 9
2.3.3- Ligaments, cartilage and articular disc 9
2.3.4- Elements 10
2.3.5- Contact 10
2.3.6- Boundary Conditions 11
2.3.7- Healthy side 12
2.3.8- Materials 12
2.3.9- Bone geometry 12
2.3.10- Screws 13
2.4. Conclusions 13
Chapter 3 - Materials and Methods 15

3.1- Introduction 15
3.2- Workflow 15
3.2.1- Mesh Preparation 15
3.2.2- Meshing 16
3.3- Prosthesis and materials 17
3.3.1- Prosthesis 17
3.3.2- Scaffold 18
3.3.3- Bone 19
3.3.4- Screws 19
3.4. Meshing 20
3.4.1- Mesh Quality 20
3.4.2- Different requirements for different instances 21
3.4.3- The UHMWPE Mesh 22
3.4.4- Non-manifold assembly 23
3.4.5- Elements 23
3.5- Contacts 23
3.6- Boundary conditions 24
3.7- Static and dynamic models 25
3.7.1- Different situations 25
3.7.2- Different models 26
3.8- Conclusions 28
Chapter 4 - Results 30
4.1- Introduction 30
4.2- MC loading 31
4.3- Stresses in the fossa component 31
4.3.1- Contact 31
4.4- Screw Loading 34
4.4.1- Normal screw configuration 34
4.4.2- Other possible screw configurations 35
4.5- Micromotion 37
4.6- Load distribution and effect on the healthy side 38
4.7- Strain in the mandible bone 39
4.8- Dynamic simulation 43
4.9- Conclusions 47

Chapter 5 - Discussion 48
5.1- The Finite Element model 48
5.1.1- MC and FOSSA_TI 49
5.1.2- Contact FOSSA_PE with MC 49
5.1.3- Screws 50
5.2- Osseointegration 52
5.3- Influence on the mandible bone and opposite side 53
5.3.1- Strain distribution 54
5.4- Limitations 54
Chapter 6 - Conclusions 57
Chapter 7 - Future Work 59
Bibliography 61
Master's Thesis file 65

Abstract

The purpose of this study is to evaluate the influence of the patient-specific TMJ prosthesis on the prosthesis components, mandibular bone, opposite joint, and mastication cycle. A finite element model was developed using the state-of-the-art techniques to model the relevant anatomical components encountered in the TMJ and the prosthesis. The contacts were modeled according to the equations of contact mechanics, the whole FE model was subjected to a convergence test, and the results were compared to the literature in order to ensure the reliability of the results. Furthermore, several tooth clenching situations were simulated to evaluate the performance of the prosthesis through commonly used parameters (e.g. maximum Von Mises stress/strain). To assess the influence of the TMJR on the remaining healthy tissue, a different FE model of a healthy patient was developed for comparison. Moreover, the implant is equipped with a scaffold that promotes osseointegration. The influence and feasibility of bone ingrowth into the scaffold was also analyzed.

Additionally, 4D CT data of the mastication cycle of the patient was used to develop a dynamic FE model of the mastication cycle. This latter model was used to observe the influence of different mandible positions on the stress in both the healthy and prosthetic joint.

The models and techniques used in this study can serve as a first step to the development of a comprehensive FE model that, with some added effort, may be considered as a virtual patient for the TMJ prostheses developed by CADskills.

List of figures and tables

List of figures

Figure 1, TMJ and its attachment with the lateral head of the pterygoid muscle [20] 2

Figure 2. Ligaments and related entities of the TMJ: sphenoid bone (1), temporomandibular ligament (2), joint capsule (3), external acoustic meatus (4), mastoid process (5), stylomandibular ligament (6), mandibular foramen (7), sphenomandibular ligament (8), anterior (a), superior (s). [20] 5

Figure 3, illustrations of the Christensen (left) [24]] and Biomet (right) [25] stock prosthesis 8

Figure 4, A.- TMJ prosthesis "Parametro Classico" from CADskills. B and C mandibular component with the enumeration of the screw holes that will be used throughout this paper 17

Figure 5, FE model of the healthy patient (left) and the healthy patient prosthetic patient (right) 17

Figure 6, Representation of the full 18 mm incisor opening (green) and of the clenching position of the mandible 28

Figure 7. Von Mises stress contours of the mandibular component in the following tasks from left to right: MAX (bone ingrowth), MAX (no ingrowth), INC, RMOL, LMOL. 32

Figure 8. (A) Von Mises and (B) Compressive stress in the fossa component for the 4 tasks. From left to right: MAX, INC, RMOL, LMOL 33

Figure 9. Contact and Von Mises stress in the 4 clenching tasks. A.- MAX B.- INC C.-RMOL D.-LMOL 33

Figure 10. Theoretical solution of the compressive, shear and Von Mises stress below the interface for UHMWPE and Ti-6Al-4V for the MAX task where the load simulated is 350 Newtons 34

Figure 11. Von Mises stress of the fossa component in the contact side with the skull bone for the 4 clenching tasks. From left to right: MAX, INC, LMOL, RMOL 34

Figure 12. Loads carried by the screws post-operative (blue) and when full bone ingrowth has been achieved (orange) 35

Figure 13. Load distribution among screws for different screw configurations. The legend reflects the number of screws that were eliminated in the simulation. Numbers in the legend indicate the range of screws that were eliminated from the simulation.....36

Figure 14. Micromotion (μm) of the mandibular component with respect to the bone. Images are shown for the tasks of MAX, INC, LMOL, RMOL from left to right. 38

Figure 15. Micromotion (in μm) of 4 cases. The numbers displayed under each case correspond with the screws removed in the simulation 38

Figure 16. Load distribution in both condyles for the prosthetic and healthy models 39

Figure 17, Microstrain along line 1 for the healthy and the prosthetic model. Keep in mind the differences in geometry observed in figure 5, only the prosthetic model is represented. Maximum microstrain in the prosthetic model reaching 840 με and 640 με in the healthy model. 40

Figure 18, Microstrains through lines 2 and 3. Both lines present in the prosthetic model. Line 2 reaching a maximum of 1120 με and line 1 824 με. 41

Figure 19. Microstrains in the posterior side of the condyle for both healthy and diseased models.....42

Figure 20, Microstrains through line 4 situated under the implant on the surface of the bone. Maximum and minimum values reached both by the case with no bone ingrowth with values of 430 and 169 με respectively. 43

Figure 21, Load transmitted by each condyle for each mouth opening.....44

Figure 22. Stress and strain contours for the dynamic model with three mouth openings: A: 5mm, B: 9mm, C:18mm.....46

Figure 23, Max Von Mises stress in the prosthesis developed by [6] (A) and the custom-made prosthesis developed by [6] (B and C). FLAT/ANAT=Flat contact surface/Anatomical fit between the mandibular component and the mandibular ramus (both Christensen prosthesis); HO/HE=Homogeneous/heterogeneous bone modeling; CSP=Custom-made condylar support prosthesis.....52

List of tables

Table 1, Mechanical properties of the materials involved in the FE model 19

Table 2, Parameters from mesh diagnosis 22

Table 3. Muscle forces for each clenching task. INC=Incisal clench; RMOL=Right molar clench: LMOL=Left molar clench; MAX=Maximum masticatory force; SM=Superficial masseter; DM=Deep masseter; MP=Medial pterygoid; AT=Anterior temporalis; MT=Medial temporalis; PT=Posterior temporalis.....29

Table 4. Values of condyle loads.....39

Table 5, Maximum, minimum and average microstrain values through lines 1,3 and 4 in the dynamic model. 45

Table 6, maximum stress and strain values for the prosthesis components and mandibular bone during 4 clenching tasks and dynamic simulation 45

List of abbreviations and symbols

TMJ	Temporomandibular joint
TMD	Temporomandibular joint disorder
TJR	Total joint replacement
FE	Finite element(s)
FEM	Finite element method
FEA	Finite element analysis
CT	Computer tomography
FOSSA_PE	The lower part of the fossa component made of ultra-high-molecular-weight polyethylene (UHMWPE)
FOSSA_TI	The upper part of the fossa component made of Ti-6Al-4V
MC	Mandibular component

Chapter 1 - Introduction

1.1- Problem statement

Temporomandibular joint disorders (TMD's) are quite common in modern society, it is estimated that approximately 25% of the world population suffers from at least one TMD [1] of which dislocation of the articular disc (see figure 1) is one of the most common [2,3]. In this particular case, surgery would not be required. However, 5% of the disorders require intervention and out of those, only 3 to 5% require invasive management [4].

When the disorder is extreme (tumor development, end-stage osteoarthritis, etc.) and surgery is necessary, total reconstruction of the TMJ may be the optimal solution. In that case, a mandibular component (commonly made of Ti-6Al-4V [5] due to its high bone integration [3] or of Co-Cr [6,7]), and a fossa component (usually made of UHMWPE [1,5,7,8]) will be implanted onto the temporal and mandibular bones respectively to take over the functions of the TMJ.

The main challenges arise when this prosthesis fails due to very high loads (which is quite rare [7]), or when it generates asymmetries in the jaw loading conditions causing the contralateral joint to be overloaded [9,10] which might lead to pain or other undesirable effects on the healthy side [1,11]. Furthermore, the TMJ prosthesis is not yet as established in the market as the hip or knee prosthesis [12] due to the early failures of the implant. The finite element method (FEM) has been shown to be a powerful tool to analyze the biomechanical behavior of the prosthesis and the structures involved in the jaw movement [1,3,5,7,9,13–15]. Furthermore, it has the potential of performing virtual tests of the TMJ, providing insightful information on the local effects arising from different loading scenarios. Additionally, given the specificity of the implant presented in this thesis, no results that appear in the literature can be extrapolated given the different design, patient, etc. Hence, FEA would provide new and unique knowledge of this implant.

The prediction of the stress distribution through the different components influenced by the TMJ is crucial for the evaluation of the design. In previous research, this

evaluation is performed through static tooth clenching simulations [6,9,16–18] with only a few considering other positions of the mandible [19]. Given the availability of 4D CT data, the prosthesis will be analyzed through different mouth openings which will provide new insights on the stress distributions on the relevant geometries. Consequently, a dynamic model will be developed through the whole range of mouth opening the patient is able to perform. This is the first study where 4D CT data is combined with FEA on TMJR research, thus it is expected to provide innovative results, so far unknown by the state-of-the-art research on TMJ replacement.

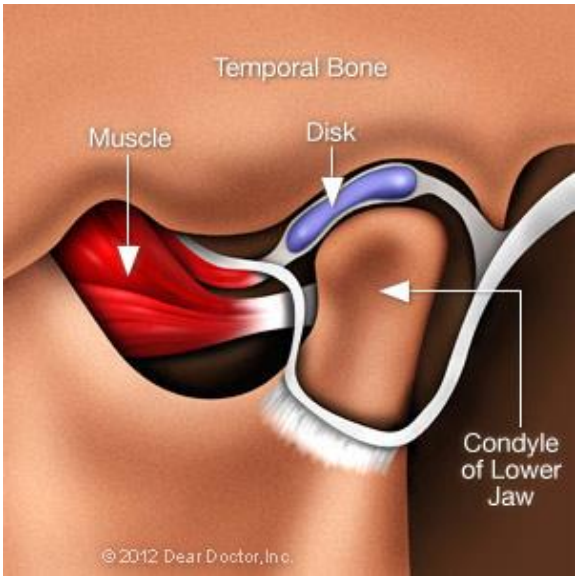

Figure 1: TMJ and its attachment with the lateral head of the pterygoid muscle [20]

1.2- Objectives

Given the possibility of failure of the implant materials [17] and the influence that the TMJ reconstruction has on the jaw mechanics [1,7,9,10], it is necessary to be aware of the local effects caused by different loading scenarios. The goal of this study is to evaluate the mechanical loads that the prosthesis will be subjected to, as well as the biomechanical influence it will have on the mastication cycle. This will be done by performing FE static analyses of different high loading scenarios the TMJ might be placed in. Furthermore, 4D CT data of the patient post-surgery will be used to establish the dynamic situations and provide new insight into the analysis of TMJ prosthesis. A FE model will be developed to obtain key parameters that will allow for a comprehensive analysis of the performance. A detailed list of objectives follows:

- Analysis of the contacts between the prosthesis' components and between implant and bone.
- Validation of the FE model with analytical results, or literature when possible.
- Evaluation of micromotion for future osseointegration of the implant
- Analysis of the loading situation of the prosthesis and contralateral joint for different mouth apertures.
- Evaluation of the fixation and load distribution among screws
- Biomechanical influence on the remaining healthy mandibular bone
- Analysis of the stress distribution on the different components and evaluation of the possible failure modes
- Provide an optimized workflow to convert SLT (stereolithography) files from segmented CT data into a FE model ready for dynamic and static simulation.

1.3- Chapters Overview

This thesis is divided into 5 chapters. The "literature review" provides the basic anatomical details influencing the joint and describes the state-of-the-art research on FE modeling of the TMJ and TMJR. Afterwards, in "Materials and Methods", the procedure followed to obtain the FE model is explained, while special focus is made on the assumptions considered necessary. Chapter 4 displays the obtained results followed by Chapter 5 where they are thoroughly discussed and analyzed. Chapter 6 wraps up this thesis presenting the conclusions obtained from the results and Chapter 7 compiles the suggestion for further research steps.

Chapter 2 - Literature review

2.1- Introduction

This chapter presents the important concepts regarding the anatomy of the TMJ and the FE model. Firstly, the anatomy of the TMJ is explained. Afterwards, a summary of the state-of-the-art in TMJ modeling is presented, while paying special attention to the modeling of the anatomical structures treated in the first section.

2.2- The Temporomandibular Joint

The temporomandibular joint (TMJ) is a bicondylar joint. In other words, the mandibular bone comprises condyles on its two ends that function at the same time [20]. Moreover, from both anatomic and functional point of view, the TMJ is one of the most complex joints in the human body due to its slide and hinge motion [21]. The hinge motion takes place when the incisor teeth separate up to (approximately) 20 mm. When the separation increases, the sliding motion takes place and the condyle slides anteriorly throughout the mandibular fossa. The TMJ is the only joint involved in mouth movements (e.g. mastication or speaking) which makes it the most used joint in the human body moving approximately 1500-2000 times per day [22].

2.2.1- The articular disc

Several entities influence the mechanics of the TMJ. Firstly, the TMJ is located between the lower mandibular bone -the mandible- and the temporal bone of the skull (figure 1 [23]). Furthermore, the peculiar characteristics of the TMJ that enable it to perform complex movements while absorbing a substantial amount of stress are provided by the articular disc (figure 2), which behaves in a viscoelastic manner as well as a shock absorber [11]. The disc also divides the joint into two sections each of which contains its own synovial membrane. In addition, the disc is attached by the collateral ligaments to the condyle medially and laterally. Due to the translation component of the condyle motion, the disc slides in and out of the socket in each movement that involves a separation of the incisors greater than 20 mm, which facilitates one of the most common TMJ disorders called “TMJ disc displacement”. Moreover, one of the functions of the disc is to increase the contact area between the

cartilaginous structures that coat both bones (the mandibular condyle and the condylar fossa), thus providing a smoother load transfer throughout the joint [11].

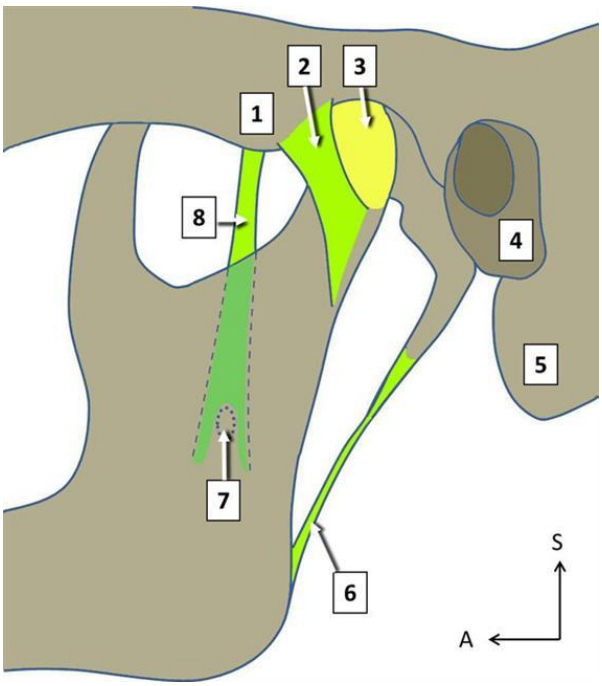

Figure 2: Ligaments and related entities of the TMJ: sphenoid bone (1), temporomandibular ligament (2), joint capsule (3), external acoustic meatus (4), mastoid process (5), stylomandibular ligament (6), mandibular foramen (7), sphenomandibular ligament (8), anterior (a), superior (s). [23]

2.2.2- Ligaments

As mentioned before, the motion of the joint is quite complex, so it requires several entities to ensure its stability. Muscles help passively and actively to keep the condyle in place, and a set of ligaments give extra (passive) stability to the joint. Furthermore, there are three main ligaments that stabilize the temporomandibular joints. They limit the range of movements the joint can reach when healthy. The main one is the temporomandibular ligament, seen as the thickened lateral part of the capsule (see figure 2 [24]). It is divided into the outer oblique portion and an inner horizontal portion. The upper part of the ligament is attached to the zygomatic process of the temporal bone and its articular tubercle, on the lower side it attaches to the lateral side of the condylar process of the lower jaw bone.

Joint dynamics are also influenced by the two remaining accessory ligaments: the stylomandibular and the sphenomandibular ligament (see figure 1). The stylomandibular ligament runs from the styloid process to the angle of the mandible and from the spine of the sphenoid bone to the lingula of the mandible which is surrounding the foramen of the mandible. There are other ligaments that offer extra stability, although, given their very small size, they are not considered when mathematically modeling the TMJ [11,15]. These are known as the oto-mandibular ligaments and they connect the middle ear with the temporomandibular joint.

2.2.3- Movements

The movements which the lower jaw can carry out are quite diverse due to the complex geometry and functioning of the TMJ. Mainly, the hinge and sliding motions allow for this wide range of movement, which is also made possible by the configuration of muscles known as the mastication muscles. These muscles act synchronously to produce the main movements studied here. As means to develop a musculoskeletal model of the jaw, it is necessary to have knowledge of the main actuators of the movement, which are: the masseter (subdivided into superficial and deep heads), temporalis (subdivided into posterior, medial and anterior heads) and the medial pterygoid muscles [1,5,9,17].

The main jaw movements and the muscles responsible for them are displayed here [25]:

- Jaw opening: mainly performed by the lateral head of the pterygoid. Since opening barely places the TMJ under any stress, it will not reappear often throughout this text

- Jaw closing: mainly performed by the superficial masseter, anterior temporalis and medial pterygoid. The situations that arise from the activation of the jaw closing muscles are the ones that usually place the TMJ under the highest stress [5,17,26].

- Protrusion: consists of driving the jaw forward and it is made possible by the lateral pterygoid. This movement cannot take place in patients where both

TMJ's have been replaced due to the loss of function of the lateral pterygoid in these patients [10].

- Retrusion: backward movement of the lower jaw. The main muscle activated for this movement is the temporalis.

- Lateral excursion: only possible if the lateral pterygoid is reattached [10].

The prosthesis used for this study is manufactured with the goal of reintegrating the lateral head of the pterygoid into the implant to regain some of the functions previously mentioned. However, since the lateral pterygoid only acts when opening the mandible to aid in the translation motion, it will not appear when discussing the jaw closing muscles.

2.2.4- TMJ replacement

TMJ disc displacement is one example of TMD that, most commonly, does not require invasive surgery. Other disorders that commonly do not require invasive surgery are extra-articular TMD's which are usually treated with the help of medication or physical therapies [3]. However, there are several disorders that can only be managed invasively, and some of them include total reconstruction of the joint. Some examples of these limit cases are: end-stage arthritis, ankyloses or tumor development [9].

Unilateral alloplastic TMJ reconstruction might produce geometrical asymmetries in the lower mandible. Nevertheless, these asymmetries produced by the unilateral reconstruction will influence the stresses that the opposite healthy joint will have to withstand [9]. Furthermore, only a few studies have been conducted where the differences in the opposite side were evaluated [1,9]. The TMJ acts as guidance for jaw movements and as a fulcrum for force generation. The loads to which the joint is subjected can cause damage to the structures inside the joint capsule which are the main factor in the development of TMD's [11]. Consequently, attention should be paid to the changes in geometry (and thus, loading) introduced by the TMJR. Moreover, the goal of the implant is to achieve the same stress and strain distribution that would take place in a non-pathological state.

2.3. The Finite Element Model

Finite Element Analysis has been widely used to study the biomechanical behavior of orthopedic devices including hip, knee and TMJ prostheses among many [9]. When validated with the in vitro testing of healthy and alloplastic TMJ TJR's the results of the FEM show a great agreement with reality [15] in both stock [1,7,10] and custom made prostheses [12]. Some of the modeling techniques presented here will be used on the geometries and 4D data obtained from the CT scans in order to develop a FE model of the implant and mandible that will be presented in the next chapter.

2.3.1- TMJ TJR research

The research performed in numerical simulations of TMJ replacement devices is overwhelmingly tilted towards stock prosthesis taking over 75% of the published research in this field. Out of these, 85% study the Christensen prosthesis, 20% Zimmer Biomet (both shown in figure 3 [16,27]) and 10% dedicated towards the Stryker prosthesis [3]. The other 25% is dedicated towards patient-specific implants, which show the novelty of this approach that was made possible mainly by the spread of 3D-printing technology.

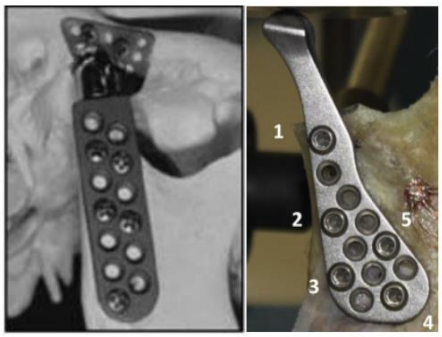

Figure 3: illustrations of the Christensen (left) [16]] and Biomet (right) [27] stock prosthesis

A patient-specific TMJ has shown to adapt better to the bone geometry, thus changing as little as possible the geometry and functioning of the jaw. Since the particular prosthesis studied here is also patient-specific (and also provided with a scaffold to promote osseointegration), it is expected to generate little stress shielding and not to deliver extreme changes in the strain distribution of the mandible bone [8].

2.3.2- Static and dynamic simulations

Up to date, all the FE analyses made of a TMJ prosthesis have been based on worst loading scenarios that take place without movement (static tooth clenching) [1,5,7,10,12,17]. The research group of A. Ramos and M. Mesnard has broadened the knowledge of the impact of TMJR by analyzing different mouth apertures captured through video recordings (after implantation [8]). Furthermore, musculoskeletal models of the human mastication cycle have been developed [15,28], whilst using healthy joints. Given the unknown impact of the TMJ replacement on the jaw dynamics, these models will not be applicable since they assume a non-pathological movement.

2.3.3- Ligaments, cartilage, and articular disc

In the interest of constructing a correct FE model of the TMJ, it is crucial to know which entities will influence the loads the joint will be subjected to. Since this study focuses on the TMJ (and as a consequence, the mandible bone), the ligaments may not be modeled without concern of altering the accuracy of the results [1,3,5–7,9,12,16,17]]. However, when modeling the whole mastication cycle, it can be advantageous to model the ligaments since they will provide additional stability. However, this approach is not common in literature since ligaments do not seem to be of great influence in the stress distribution in the joint [15]. The constraints introduced by these ligaments can be substituted with fixed constraints on the mandibular condyle to reduce the computational load of the simulation.

In addition, the cartilage structures residing inside the joint capsule are shown not to influence the stress distribution, since they just transmit the loads from the disc to the bone without suffering notable deformations [15]. However, the articular disc has a great influence on the load transfer from the condyle to the mandibular fossa. Given its viscoelastic behavior, it transforms the compressive stresses into shear stresses by increasing the contact surface between the cartilaginous structures. Thus, decreasing the overall stress withstood by the bones and cartilage [11].

It may be an advantage to model the disc for the biomechanical analysis of the mastication cycle. The articular disc enables distribution of local contact stresses over a much wider area of the very incongruent articular surfaces by transforming

compressive principal stress into shear stress [28]. However, it is not trivial that the dynamic simulation sees influence from the articular disc [9]. Moreover, during static analysis, the behavior of the disc is of lower importance since it acts as a load transfer between the condyle and the temporal bone. As long as the stresses in the interfaces of the bones do not need to be known, the disc is not necessary since it only acts as a shock absorber and load distributer between the condyle and the temporal bone [11].

It should be known that particularly shear stresses are believed to alter the cells, thus damaging the disc. If the damage of the disc is needed to be accurately modeled, the shear stresses transmitted between the bones need to be monitored accordingly [28]. On the other hand, compressive stresses do not have such an impact on the disc's health [15], although as previously mentioned, a strong increase of load in the healthy joint will affect the patient negatively and should be avoided [1,11].

2.3.4- Elements

In order to obtain a realistic result, proper meshing of the geometries is crucial. In previous research, the overwhelming majority of FE analyses of the TMJ prosthesis, the joint or the whole mandible uses tetrahedral elements since complex geometries are easily meshed with these type of elements [5–7,12,15,29,30]. Tetrahedral elements require higher computational resources since they are more space inefficient than hexahedral elements due to the highly unstructured meshes they produce. However, the meshing of complex structures (curved edges, acute angles) is sometimes not possible with hexahedral elements. Further discussion of elements can be found in the following chapter. Furthermore, contact elements must be used in the interfaces between bone-bone, bone-implant, and implant-implant.

2.3.5- Contact

The focus will be placed on the interfaces between the entities of the model since they provide crucial information. For instance, accurate contact modelling will provide knowledge on whether the fossa component of the prosthesis will be subjected to abrasion if the stress produced by the contact with the condyle component is not above a certain threshold [5], or whether there will be bone ingrowth, which in turn improves the interface strength between the implant and the bone [31]. For these reasons, special attention is given to the contact conditions in this particular

prosthesis. In most of the FE analyses performed up to date, the contact between the entities present in this simulation (bone, UHMWPE, Ti-6Al-4V, articular disc) is simulated with the Coulomb friction model which is assumed to not introduce any inaccuracies in the loading conditions present here [29].

2.3.6- Boundary Conditions

The boundary conditions vary with the task being simulated. For instance, the static analysis of the mastication of a specific food type will set the boundary conditions differently depending on the foods being analyzed [32]. Furthermore, the most commonly used boundary condition in fixing the vertical displacement of a selection of teeth (molars, incisors, etc) in order to simulate tooth clenching, which has been assumed to produce the worst loading situation for the implant and healthy TMJ [1,12,17]. However, this notion will be challenged here, since there is the possibility of testing multiple mouth apertures.

Additionally, there is an agreement in literature where the skull is fixed [5–7,12]. This assumption allows for strong simplification of the FE model given the removal of most of the skull bone.

The jaw closing and opening muscles forces are commonly applied in the 3D model at the muscle attachment points in the jaw obtained from literature [9,17] for the static simulations. On the other hand, the dynamic situation needs a model that provides the force and direction of the muscle for different mouth apertures and different tasks. For these situations, normally a Hill-like model is used [15] where the muscle force is computed as the sum of a passive and an active component. However, when the small mouth apertures are considered (this is the case given that patients with a TMJ TJR have limited range), the muscle forces are often assumed to be constant and maximal, given the short variation in length they will experience [8]. Moreover, the direction of the muscle forces needs to be accurately modeled since they have been shown to have a great influence on the loading transmitted through the condyles [33].

There is a substantial amount of research done where the forces applied during tooth clenching are measured. However, normally, these forces are measured during a static analysis through EMG, MRI [7,34], or performing static optimization of a musculoskeletal model [15] or a combination of both [34].

2.3.7- Healthy side

Little research has been published regarding the influence of the prosthesis on the healthy side of the joint. However, there is a consensus that a healthy mandible withstands lower stresses in the TMJ - particularly in the articular disc - than the contralateral side of the mandible that has gone through a total alloplastic surgery in one side (especially if the prosthesis is not custom-made [8]). However, it has been shown, in numerical models, that the healthy side is positively affected by a 15% decrease in stress in the articular disc [1], after the surgery, since the physiological joints in a pathological model were not performing as in the healthy model. Nonetheless, when comparing the load on the contralateral side on a patient that has undergone total TMJ reconstruction with the load on a condyle of a healthy patient, the load increase is approximately 15% when using a stock prosthesis [9]. Furthermore, increases in mechanical loads have been shown to produce cartilage and articular disc damage [15], therefore it is crucial for the implant not to overload the contralateral side.

2.3.8- Materials

The most used materials for the TMJ prosthesis are Titanium-Aluminum-Vanadium alloy (Ti-6Al-4V) and Cobalt-Chromium-Molybdenum alloy (Co-Cr-Mo) for the mandibular and fossa component given that both are biocompatible and have high yield stress. There is a tendency in the latest custom-made prosthesis to use Ti-6Al-4V as the main metal component given that it is feasible to 3D-print which makes it appropriate for patient-specific implants [5]. In addition, it will induce lower stress shielding compared to Co-Cr-Mo due to its lower stiffness. Furthermore, the scaffolding used in this prosthesis will significantly reduce the stiffness and promote osseointegration which will, in turn, reduce the load of the screws over time and reduce the stress shielding even further due to the transferring of the load from the screws to the prosthesis.

2.3.9- Bone geometry

The geometry of the bone components used is the same as previously used to make the custom-made design. In most cases, it comes from CT scans [1,11,15,16] which allows to know the bone distribution (trabecular vs. cortical bone), thus assigning

different mechanical parameters to each [16]. However, as it was previously mentioned, this improvement will not significantly change the results [35] and will increase the computational resources needed.

2.3.10- Screws

The screws are a necessary component of the prosthesis especially right after implantation. They will keep both parts of the implant fixed to the bone until a substantial amount of bone has ingrown into the implant. In literature, some groups focus on the stresses endured by the screws [5,12] and others do not take their exact geometry into account [16,17]. Given that screws are made of metal (and not of UHMWPE, like the fossa component), they can withstand much higher loads. In previous studies, where custom-made prostheses were analyzed, it has been shown how the stress withstood by the screws stay (generally) below 20% their yield strength [5,6].

2.4. Conclusions

In this section, several entities have been shown to have an influence in the joint (e.g. ligaments, muscles, articular disc), and also, how several research groups take care of the constraints these entities introduce. To summarize:

- Ligaments are generally excluded from the simulation and substituted by fixed constraints which have been shown not to introduce notable changes in the loading of the TMJ.
- The contacts between the different entities (physiological or artificial) are simulated with the Coulomb model of friction. There is good documentation in literature of the coefficients of friction between the different entities.
- The forces exerted by the muscles and their direction are in literature for different clenching tasks.
- There is a general agreement on the boundary conditions. The skull needs to be fixed over the zygomatic arch. In addition, the screws are not necessary to be simulated since they are not expected to fail, provided a proper screw configuration in the mandibular component.
- It is not necessary to assign different mechanical properties to bone given that its distribution does not affect the overall load endured by the joint.

- There is a consensus in literature that the elements used should be tetrahedrons. However, a choice on whether they are linear or quadratic should be made.
- The disc provides a wider contact area between bones. It is necessary to model if the accurate stresses in this interface need to be known. However, if only the damage to the disc or the load endured by the joint needs to be known, it will not be indispensable to be modeled.
- The teeth have little influence on the mandible, in particular on how condyle behaves so they can be excluded from the model.

Chapter 3 - Materials and Methods

3.1- Introduction

This chapter will thoroughly explain the steps followed to obtain the FE model of the mandible with and without the implant. Hence, it will include the software used for image processing, meshing, and calculations. However, the image acquisition process related to the CT scans and segmentation will not be discussed in depth since it falls outside of the scope of this thesis. The focus will be placed on the used workflow and the assumptions made to develop the FE model. In the last section of the chapter, the differences between the static and dynamic model will be explained.

3.2- Workflow

3.2.1- Mesh Preparation

As mentioned in the previous chapter, the geometries of the patient's anatomy were obtained from CT scans. However, these CT scans contain unnecessary geometries that should not be included in the FE model (e.g. artifacts from the image acquisition system, teeth, which were shown to be unnecessary for the simulation [34,36], or most volume of the skull). Furthermore, all the geometries that need to be included in the simulation need to be meshed for the FE calculations. This operation removes every detail that is smaller than the element size used. Since the interest is mainly focused on the implant, the mandibular bone's mesh will not be as refined as the implant. However, it should be noted that the decision is taken mostly because the volume of bone exceeds the volume of the implant substantially. Hence, if everything was meshed with the same accuracy, the computational cost of the simulation would increase substantially. Further discussion will appear in the meshing section of this chapter. Consequently, there is a need for an image processing software that allows for the removal of unnecessary artifacts from the image acquisition process and smoothing of surfaces with unnecessary detail.

The software used to pre-process the image data was Meshmixer from Autodesk thanks to its simplicity and intuitive interface. The work performed here had mostly to do with the mandible bone given the abundance of detail that is required in the

interface with the implant and the lack of it needed in the rest of the bone. A high degree of accuracy of the results can be achieved with a coarse mesh given that the exact geometry of the jaw bone is not interesting. The results of all the meshes used were later validated with a mesh of half its element edge length (which increases the number of elements by an approximated factor of 10) obtaining results that differed in less than 2% in maximum and average Von Mises stress, maximum and average Von Mises strain, and displacement in each of the components. The fact that a lower density of elements can be used in the bone without a decrease in reliability of the results allows for the geometry to be smoother. Overall, Meshmixer was used to perform image processing on the bones (mostly on the mandible) to allow for an efficient meshing in the next step of the workflow.

3.2.2- Meshing

The prosthesis evaluated here is the "TMJ-TJR Parametro Classico" (shown in figure 4, patient-specific design). A 3D FE model of the jaw, the lower part of the temporal bone with the mandibular fossa, and prosthesis components need to be created. Furthermore, a healthy jaw will also be modeled from a different patient whose CT scan is also available. For this healthy case, only the jaw and the mandibular fossa will be modeled (see figure 5). After the pertinent mesh preparation steps have been taken in Meshmixer, the next step in the workflow consists of meshing the geometry. This will take place in the 3-Matic 12.0 software from Materialise, since it provides additional image processing tools which have added value to the ones available in Meshmixer. Furthermore, 3-Matic provides several algorithms for meshing 3D geometries efficiently. Due to the previous step where the geometry was smoothed, there are no sharp edges or unnecessary details in the bone geometry. Consequently, the meshing algorithm will run smoothly creating a high-quality mesh. The meshing requirements will be discussed further in this chapter.

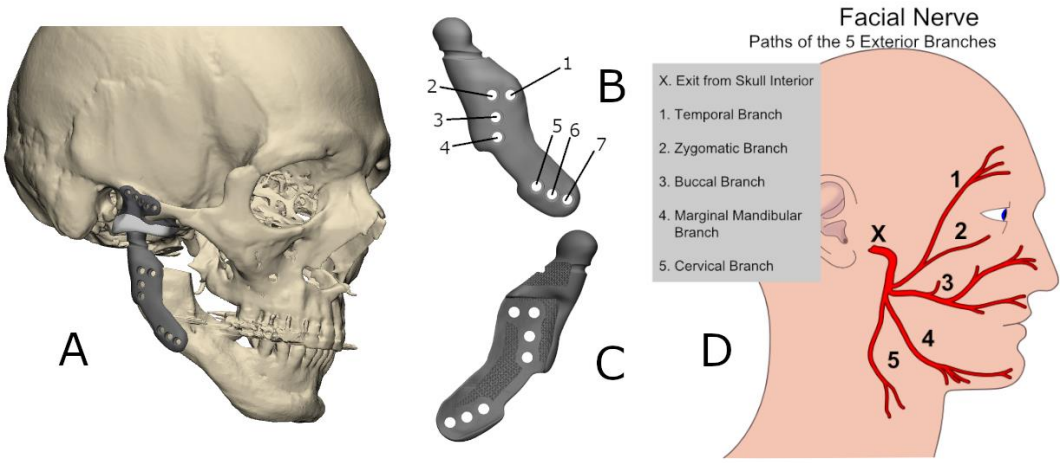

Figure 4: A.- TMJ prosthesis "Parametro Classico" from CADskills. B and C mandibular component with the enumeration of the screw holes that will be used throughout this paper. D.- Display of the 5 branches of the facial nerve [37]

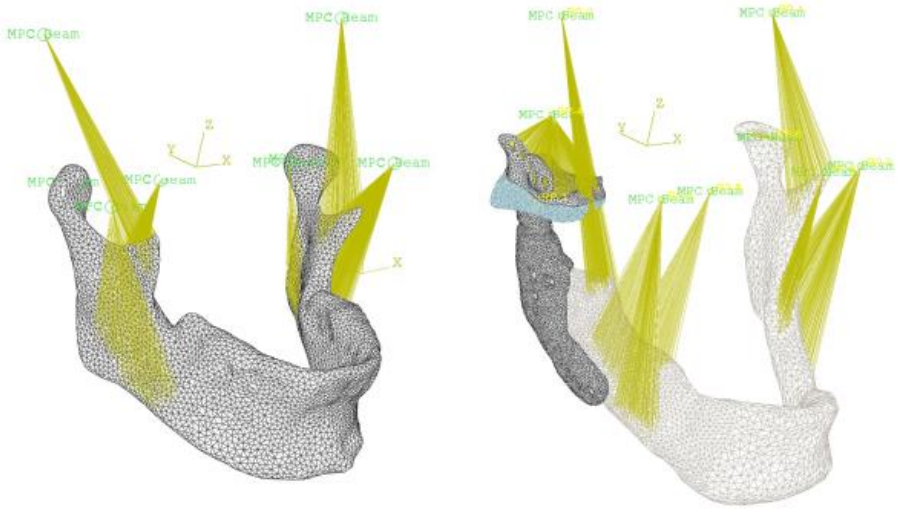

Figure 5: FE model of the healthy patient (left) and the prosthetic patient (right). Yellow lines indicate the constraints joining the muscle attachments.

3.3- Prosthesis and materials

3.3.1- Prosthesis

The prosthesis is made of three components (see figure 4): the lower part of the fossa component (FOSSA_PE) which is made of UHMWPE, the upper portion of the fossa component (FOSSA_TI) and the mandibular component (MC) which are both made of Ti-6Al-4V. Furthermore, the mandibular component can be subdivided into its solid part and the scaffold. Given that Ti-6Al-4V has a much higher stiffness than bone (see

table 1) it will produce stress shielding when loaded. For this reason and to promote bone ingrowth into the implant, a scaffold is placed to occupy most of the contact with the bone. Once osseointegration of the implant has occurred, it is expected for the bone to carry most of the load, thus decreasing the stress shielding produced by the implant. The mechanical properties of the materials (table 1) are obtained from the providers of each material with exception of bone (which is obtained from literature [5,12,38] and the scaffold which was estimated by analyzing research made on scaffolds with similar geometries and materials [39]).

Additionally, the contact between both components of the prosthesis is facilitated using UHMWPE in the bottom side of the fossa component to ease the sliding motion and decrease friction. This approach has been used in most of the more current TMJ prosthetic designs [5,9]. In this implant, friction is greatly reduced using DLC coating on the contact surface of the mandibular component. That way the risk of wear is reduced on the UHMWPE which has been shown possible when simulating clenching tasks [5].

3.3.2- Scaffold

The scaffold is a fundamental component of the prosthesis. It is expected it will provide the conditions necessary for the bone to grow inside the implant, and thus allowing the bone to carry most of the load that way reducing stress shielding and screw loading. The specific scaffold used here is of type diamond 20 (1,35 mm) produced by Materialise.

Promoting bone ingrowth is the main function of this scaffold. It has been shown that the strains the bone is subjected to have to be under a specific threshold. There is no consensus on this limit of micromotion that may be admissible to achieve bone ingrowth. Some authors have revealed the limit lies over 100 μm [40,41] while others state around 40 μm [19]. However, in this study, the limit will be taken as the most conservative found in the literature which corresponds to a maximum of 28 μm [17]. Furthermore, low micromotion is also desirable for the stability of the prosthesis, given that too much motion will lead to loosening of the screws and thus failure of the implant. However, it can be assumed if the micromotion is low enough to promote osseointegration (with the most conservative requirement) loosening of the screws will not take place.

3.3.3- Bone

The mechanical properties of bone depend widely on age, nutritional state, bone-related diseases, etc. [39]. For this reason, substantial research has been performed evaluating the behavior of bone (trabecular and cortical) under loading. Furthermore, as mentioned previously, the distribution of bone density does not influence the results of the simulations. Therefore, the values taken for the mechanical properties of bone (shown in table 1) are according to several references [5,12,38]. Furthermore, the bone introduced in this simulation has been considered isotropic and linear given the load range it is subjected to. Its viscoelasticity has not been considered either.

Table 1: Mechanical properties of the materials involved in the FE model [9,12,17,38,39]

Material	**E (MPa)**	**ν**	**Elastic yield limit**
TI-6Al-4V	113000	0.3	1301 MPa
Cortical Bone	15000	0.3	4000 $\mu\varepsilon$
Scaffold	9000	0.1	0.01 ε
UHMWPE	683	0.46	22.2 MPa

3.3.4- Screws

Throughout this research, two situations are considered. The first one right after the operation (post-operation) where it is assumed that the only fixation between the implant and the bone is through the screws. The second situation takes place when the bone is assumed to have grown into the scaffold and thus, the interface is rigid (with the same stiffness as the bone) not allowing slip between them. For the first situation, only the maximum loading will be explored given that it is assumed the prosthesis will have to withstand these specific boundary conditions during the first weeks after implantation. For the fully ingrown prosthesis, all 4 clenching tasks and dynamic analysis will be performed. The loading for the clenching tasks is shown in table 3 where the forces from the muscles of mastication are obtained from literature [17,34]. Furthermore, in order to truly estimate the worst case scenario (when the screws are being evaluated), it is assumed the MC does not make contact with the roof of the osteotomy platform, that way the MC is fully supported by the screws (or

scaffold in the case of osseointegration). This scenario is not considered when the strains in the bone are calculated since the osteotomy platform is expected to withstand a substantial amount of stress from the vertical forces.

The bone ingrowth into the implant is expected to substantially decrease the load taken by the screws. In addition, screws are thoroughly studied in previous research on TMJR's. Furthermore, physiological loading has been shown not to be high enough to reach yield stress in these structures [6,14,16,17,42], given the high yield strength of Ti-6Al-4V (see table 1). Moreover, loads in patient-specific prostheses are shown to be lower than in stock prosthesis [7,8]. Consequently, it has been considered unnecessary to model the whole geometry of the screws mainly because of the a priori knowledge on the safety of those structures under the conditions used in this study. Assuming that the maximum stress in the screws will not be close to the yield strength of Ti-6Al-4V, one may consider the possibility of fatigue failure which would take place under lower absolute loads. Nevertheless, bone ingrowth is expected to happen and will be analyzed as a parameter of performance on the implant. Therefore, the loads on the screws will be greatly reduced shortly after implantation making failure by fatigue of these structures unnecessary to be considered. The mechanical influence of the screws will be modeled in order to obtain knowledge on the performance of the design and influence on bone ingrowth. Additionally, the load will provide a starting point that, with some assumptions (like pure shear loading in the screws), the maximum stresses on the screws can be approximated.

The top three screws of the MC might be closely positioned to the left marginal branch of the facial nerve as seen in figure 4D. In order to avoid causing nerve damage, it may be useful to remove these screws as long as the stability of the MC is not compromised. This situation will be evaluated analyzing the load taken by the bottom screws and its influence on micromotion between the MC and the bone.

3.4. Meshing

3.4.1- Mesh Quality

Meshing is a highly important part of any FE project. A bad quality mesh guarantees unreliable results. An important portion of the research has been invested in developing the best possible meshes. There are parameters available that help to

diagnose the quality of the mesh (displayed in Table 2). The minimum or maximum value for each parameter is obtained via the Abaqus mesh quality checks, except the aspect ratio which has been added as it is commonly used to diagnose distortion of the FE. As shown in Table 2, the diagnosis of the meshes is satisfactory in every evaluated parameter except in the aspect ratio (which is also considered a conservative value) in which approximately 1% of the elements in all the instances have an aspect ratio higher than 10. However, a quick inspection of these elements shows that they are positioned mostly inside the volumes and not in areas where stress concentrations, or failure zones are expected (e.g. contact side of the fossa, screw holes, the contact surface between bone and implant…).

3.4.2- Different requirements for different instances

There are several instances in the model which will require different element sizes. For instance, the areas where high contact stresses take place (between the MC and the fossa component), require a great mesh refinement as a consequence of the non-linearity of the contact and its low stability due to the complex geometry and the difference in stiffness between the Ti-6Al-4V and the UHMWPE. Moreover, as previously mentioned, the mandible does not require a high level of refinement since there will not be stress concentration throughout the bone. Additionally, the Ti-6Al-4V component of the fossa does not need a high refinement of the mesh given that there will be no concentration of stresses given that the fossa is custom-made for this patient [5,8]. It will be shown that the screws in the fossa component are not subjected to high stress since most of the compressive load is transmitted through the contact from the Ti-6Al-4V and the bone (due to the custom fit of the implant). Given this transmission of compressive stress the FOSSA_TI will not need further refinement.

Table 2: Parameters from mesh diagnosis

Models	Parameters					
	Minimum face angle (degrees)	**Abaqus shape factor**	**Maximum face angle (degrees)**	**Aspect ratio**	**Number of elements**	**type of element**
Max/min value	5	1.00E-04	170	10		
Healthy skull	6.28	0.0015	156.6	1%	50553	C3D4
Healthy jaw	13.86	0.017	151.83	1%	23373	C3D4
FOSSA_PE	13.86	0.0216	144.6	1%	88930	C3D4
FOSSA_TI	14.78	0.02	96.03	1%	6177	C3D10
MC	9.61	0.018	146.43	1%	29109	C3D10
Unhealthy jaw	6.68	0.0003	164.46	1%	29109	C3D4

3.4.3- The UHMWPE Mesh

Given the specific geometries of the components of the prosthesis (due to its patient-specific nature) the contacts produced by their interaction is complex. It has been shown that the geometry of the lower surface (which is in contact with the MC) of the fossa component heavily influences the load transfer through the prosthesis [19]. Hence, the geometry of the UHMWPE, specifically the lower surface, must be preserved as accurately as possible throughout the meshing process.

Additionally, given the nature of the contact between the MC and the FOSSA_PE where the former is several orders of magnitude stiffer than the latter, the mesh of the FOSSA_PE should be further refined to avoid residual penetration during the simulation. This is due to the way Abaqus solves for the contact between surfaces allowing for some penetration of the master surface in the slave surface, which will produce convergence errors if the slave surface is too coarse given that the penetration will be much larger than the displacement (tolerance) allowed to the master surface.

3.4.4- Non-manifold assembly

As it was previously mentioned, the screws will not be simulated in this study. This assumption can be made without compromising the reliability of the results due to the feature available in Mimics 12 of non-manifold assembly. The nodes in the interface of the two components (MC and bone) are matching. Moreover, this will allow a good approximation given the fact that the nodes that would be in contact with screws will have matching degrees of freedom. The movement of one node in the MC will be replicated by the movement of the closest node (which because of the non-manifold assembly will be in the exact same position) of the bone achieving this way a good approximation of the overall strains the screws would produce in the implant and bone.

3.4.5- Elements

It has been shown that for bone structures, which generally have highly irregular geometries, a tetrahedral mesh is a better approach than a hexahedral mesh [30]. For the prosthetic components, quadratic elements will also be used, given the stress concentration (that is expected to surround the screws and contacts) are predicted to be better modeled with higher order elements [16]. Moreover, contact elements (C3D8H) will be used in the interface surfaces of the contacts since contacts cannot be solved with C3D10. So quadratic elements are used for the implant and bone due to the higher accuracy when describing the geometry and stress concentration and contact elements will be used in the interfaces between the components.

3.5- Contacts

The correct modeling of the contacts is crucial in this study. The situations that are of any interest tend to take place in the interface between components. Some examples are bone ingrowth and micromotion taking place between the scaffold and the bone, high concentration of stress in the contact between the FOSSA_PE and the MC or compression and shear stresses between the two fossa components. Each of these contacts has different characteristics and thus, they are be modeled differently.

The fossa component is put together through thermal pressing of the FOSSA_TI and FOSSA_PE. This contact will be modeled as “hard” in the normal direction and “rough”

in the tangential direction which means that both penetration and slip between components will be constrained. Furthermore, no separation of the two components is allowed. These constraints allow for compressive, tensile and shear stresses to be transmitted through the interface of the components. This is the main advantage of modeling the components of the fossa separately.

An important characteristic of this implant is the stimulation of osseointegration of the MC. The bone ingrowth will not allow slip between the MC and the bone once it has had the chance to grow inside the implant. However, as mentioned previously, there will be no ingrowth right after implantation and all the load will be carried by the screws. Needless to mention, this is the worst scenario for the screws since all the load transmitted by the prosthesis will be carried by them (assuming no contact with the osteotomy platform). The evolution of the screw loading produced by the bone ingrowth will be evaluated (the decrease in loading in the screws and the increase in loading in the bone). Maximum force during tooth clenching will be studied with and without bone ingrowth. Nevertheless, to accurately model this situation, the interface between the bone and the scaffold (and solid implant too, given that not all the contact between bone and MC is scaffold) has to be accurately modeled for the stress shielding effect of the implant and the screw and bone loading to be properly approximated. Right after implantation, the interface between Ti-6Al-4V and bone will be modeled as hard contact (no penetration) with the Coulomb model of friction. Furthermore, the specific friction coefficient for this contact will be estimated with 0.3 [1,6]. Additionally, when the bone is assumed to be fully integrated into the implant, this interface will be assumed to be elastic allowing no slip of the components. The stiffness of this interface will thus be the stiffness of bone (Table 1).

3.6- Boundary conditions

The proper setting of loads and boundary conditions is highly important to properly model the load transfer that takes place throughout the TMJ [33]. The magnitude and direction of the loads are obtained from the literature [17,34]. The loading conditions include the muscles of mastication: superficial masseter (SM), deep masseter (DM), medial pterygoid (MP), anterior temporalis (AT), posterior temporalis (PT) and middle temporalis (MT). They have been shown in multiple studies that they recreate the loading conditions of the closing of the mandible accurately [5,6,8,16–18].

Furthermore, the forces exerted by these muscles vary from task to task. This is shown in Table 3 which presents the different loading of each muscle by the task.

The boundary conditions are set in the pertinent teeth depending on the task. All of them are displayed in Table 3. As previously mentioned, the skull has all of its degrees of freedom constrained. Additionally, the specific ligaments are not modeled since they would bring unnecessary complexity to the model. The healthy condyle is constrained by the temporal bone which does not allow it to move up. The lateral degree of freedom is also constrained so it cannot dislocate laterally (a movement that would be prevented by the ligaments). Rotation and dorsoventral movements are allowed since it is necessary for the sliding motion of the condyle.

The articular disc is another fundamental instance of the TMJ playing an important role in increasing the contact surface between the condyle and the glenoid fossa. However, in this study, the specific stress distribution in the contact site between the healthy condyle and the fossa is not of great interest. Instead, the focus is placed on the contact site between the MC and the FOSSA_PE given the fact that it has been shown to be a problematic area where high stresses arise [5]. When the influence of the prosthesis on the healthy side is evaluated the main parameter of interest is the load transferred from the condyle to the bone through the articular disc without the need of modeling the actual behavior of the disc. An increase of this load will increase the risk of damage of the disc and that is where the interest resides when modeling the influence of the TMJ prosthesis on the healthy side [8,15]

3.7- Static and dynamic models

3.7.1- Different situations

To evaluate the performance of the prosthesis, different clenching situation are evaluated. The focus will be placed on the strains produced in the bone and in the stress the components are subjected to. The results obtained for each component will be compared with the values of other patient-specific implants in literature and the strains induced in the bone will be compared with the healthy model set up with the same loading and boundary conditions. The conditions used are shown in Table 3 where the forces of each muscle for different tasks are shown: Incisal clench (INC) right unilateral molar clench (RMOL), and left unilateral molar clench (LMOL). These

are assumed to be the most demanding tasks which the replaced and healthy joint will undertake during daily usage.

To further challenge the prosthesis a fourth (fictional) clenching task is introduced. The maximum forces exerted by each muscle are compiled into the task called MAX. Given the highest possible force exerted by each muscle is on display in this simulation, it can be assumed that a prosthesis that can withstand this condition will not fail under normal daily life conditions (without taking fatigue into account).

3.7.2- Different models

Three models have been used to study the behavior and biomechanical influence of the prosthesis. Firstly, a static and diseased model has been used in order to evaluate what has been documented as the worst possible physiological loads (shown in Table 3), which appear when the mouth is fully closed in the situation called "tooth clenching" [5,17]. The data to form this model has been taken from a single CT scan of the patient already implanted with the prosthesis. Consequently, no adjustment of the prosthesis has been needed, given the fact that the components are in their final post-surgery positions (no alignment needed). As previously mentioned, 4 tasks were simulated which will provide a broad range of information on the loading conditions of the prosthesis. This enables a comparison of the influence the prosthesis has on the healthy side, and also the stresses that the materials will need to withstand.

A second model from a (different) healthy individual is also created. The situations, in this case, will be different since every human has a different jaw (as observed in figure 5). However, highly useful information can be extracted from the strains and loads that can be observed in healthy tooth clenching situations. In previous research, the strong influence of the prosthesis on the healthy condyle loading (especially in stock prosthesis) has been shown, where in some cases, the increase in loading reached 115% of the normal situation [9]. Also, the strain distribution surrounding the implant will be compared to the healthy model in order to evaluate stress shielding.

Finally, thanks to the innovative 4D CT scan technology available, a model from the patient that has undergone TMJ reconstruction is developed for different jaw positions. This type of real data has not been available for long and it has never been

implemented in research on TMJ prostheses. The simulation ran with this data will include a normal mastication cycle where the patient is simulating crunching food with his molar teeth. The food is considered very hard in order to evaluate the worst case scenario (and also obtain maximum muscle activation). Additionally, it should be mentioned that this patient is not able to separate the incisor teeth more than 20 mm (approximately) as commonly observed in patients with a total TMJR. Furthermore, the 4D data is expected to bring added value to the field of research since the only simulations where a TMJ implant has been positioned with the mouth open were modeled through video recordings of the mandible position [8]. The smallest and greatest mouth openings are shown in figure 6 where both mandibles are superimposed.

Since the same FE model is used for the dynamic simulation, most of the assumptions made from the static model will still be made here (screws, ligaments, muscles, mechanical properties, etc.). However, it should be noted that the boundary conditions will change slightly due to the opening of the mouth. The directions of the muscle forces will slightly vary, and the boundary conditions will be placed in the molar teeth (in both sides) in order to simulate the crunching of hard food which induces the highest muscle activation. To model this change of direction the muscle fibers, the attachments in the skull are introduced, that way the loading direction will be easy to extract from the FE model. The muscle attachments in the skull have been obtained from the CT scan of the patient.

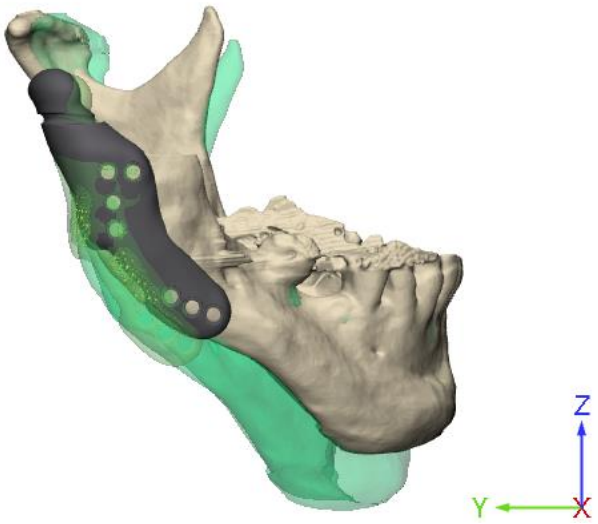

Figure 6: Representation of the full 18 mm incisor opening (green) and of the clenching position of the mandible

3.8- Conclusions

In this chapter, the methodology followed to obtain the FE model of the mandible and the prosthesis is presented. Several assumptions are made with the purpose of removing unnecessary complexity from the model. The most notable of these assumptions are: simulation of the mechanical influence of the screws instead of the definition of their 3D geometry, the substitution of the ligaments for boundary conditions with the same influence and removal of small details of the bone, modeling of the risk of damage of the articular disc by overload of the contralateral joint and Coulomb friction model used for the contacts and maximum muscle activation for static tooth clenching. Furthermore, it is also explained how the areas of interest (e.g. contacts among prosthesis components, bone-implant contact) are modeled. The boundary and loading conditions are presented as well as the models that will be used in the analysis. The next chapter presents the results obtained when applying these loading scenarios to the FE models.

Table 3: Muscle forces for each clenching task. INC=Incisal clench; RMOL=Right molar clench: LMOL=Left molar clench; MAX=Maximum masticatory force; SM=Superficial masseter; DM=Deep masseter; MP=Medial pterygoid; AT=Anterior temporalis; MT=Medial temporalis; PT=Posterior temporalis

Clenching Taks	Side	Direction	Muscular force (N)						Constraint
			SM	DM	MP	AT	MT	PT	
INC	**Right**	**Force**	76.2	21.2	136.3	12.6	5.7	3.0	Incisor teeth
		Fx	-15.8	-11.6	66.2	-1.9	-1.3	-0.6	
		Fy	-31.9	7.6	-50.8	-0.6	2.9	2.6	
		Fz	67.4	16.1	107.8	12.4	4.8	1.4	
	Left	**Force**	76.2	21.2	136.3	12.6	5.7	3.0	
		Fx	15.8	11.6	-66.2	1.9	1.3	0.6	
		Fy	-31.9	7.6	-50.8	-0.6	2.9	2.6	
		Fz	67.4	16.1	107.8	12.4	4.8	1.4	
RMOL	**Rigth**	**Force**	137.1	58.8	146.8	115.3	63.1	44.6	Right molars
		Fx	-28.4	-32.1	71.3	-17.2	-14.0	-9.3	
		Fy	-57.4	21.1	-54.8	-5.1	31.6	38.1	
		Fz	121.2	44.6	116.1	113.9	52.8	21.1	
	Left	**Force**	114.2	49.0	104.9	91.6	64.1	29.5	
		Fx	23.6	26.8	-51.0	13.6	14.2	6.1	
		Fy	-47.8	17.5	-39.1	-4.0	32.1	25.2	
		Fz	101.0	37.1	83.0	90.5	53.7	14.0	
LMOL	**Right**	**Force**	114.2	49.0	104.9	91.6	64.1	29.5	Left molars
		Fx	-23.6	-26.8	51.0	-13.6	-14.2	-6.1	
		Fy	-47.8	17.5	-39.1	-4.0	32.1	25.2	
		Fz	101.0	37.1	83.0	90.5	53.7	14.0	
	Left	**Force**	137.1	58.8	146.8	115.3	63.1	44.6	
		Fx	28.4	32.1	-71.3	17.2	14.0	9.3	
		Fy	-57.4	21.1	-54.8	-5.1	31.6	38.1	
		Fz	121.2	44.6	116.1	113.9	52.8	21.1	
MAX	**Right**	**Force**	190.4	81.6	146.8	154.8	91.8	71.1	Molars
		Fx	-39.4	-44.6	71.3	-23.1	-20.4	-14.8	
		Fy	-79.8	29.2	-54.8	-6.8	45.9	60.8	
		Fz	168.3	61.9	116.1	152.9	76.8	33.7	
	Left	**Force**	190.4	81.6	146.8	154.8	91.8	71.1	
		Fx	39.4	44.6	-71.3	23.1	20.4	14.8	
		Fy	-79.8	29.2	-54.8	-6.8	45.9	60.8	
		Fz	168.3	61.9	116.1	152.9	76.8	33.7	

Chapter 4 - Results

4.1- Introduction

In this section, the results obtained from the FE model will be displayed. The focus will be placed in the stress and strains in the prosthesis and the bone, while also taking care of the possible failure zones of the implant. The biomechanical influence of the TMJR on all the structures that directly interact with it (contact) is thoroughly explored with parameters that aid in the understanding of the differences with a healthy TMJ.

The biomechanical performance of the TMJ prosthesis can be evaluated in several ways. There are some parameters available in the literature that are commonly treated as standards in research related to this kind of prosthesis. They include relative micromotion between the mandibular component and bone (to evaluate stability and osseointegration), maximum Von Mises stress in the mandibular and fossa component, maximum stress and strain in the mandibular bone and healthy condyle [6,7,16–18]. Furthermore, when evaluating the performance of the prosthesis, it is useful to compare its effects with a healthy model. That is why a completely healthy jaw (no signs of TMJ disease) was set up with the same loading conditions.

As previously mentioned, the geometries of the screws are not accurately modeled. Hence, the exact stress distribution on them will not be known. However, the load each screw will carry can be modeled, and afterwards, can be used to estimate the maximum stress if the loading condition is known. Additionally, the expected decrease in loading is shown when bone ingrowth is fully developed inside the prosthesis and the strain distribution between right after implantation (no ingrowth) and after bone ingrowth is evaluated.

Out of the three components of the prosthesis (MC, FOSSA_PE, FOSSA_TI) the UHMWPE has been shown to be the material working closest to yield strength during clenching situations [5], especially the small contact surface between the MC and the FOSSA_PE. The results obtained of this surface will be validated with the equations of

contact mechanics in order to obtain reliable results on the conditions the UHMWPE is working on.

4.2- MC loading

As seen in figure 7, the Von Mises stress in the MC is much lower than the yield stress limit of Ti-6Al-4V. Furthermore, the only situations where the 150 MPa is reached by the MC component is in the case maximum masticatory force (MAX) and right molar clench (RMOL), where the Von Mises stress is 169 and 153 MPa respectively. Consequently, it can be assumed that the MC will not fail under physiological loading. Moreover, this stress is located at the corner under the fourth screw, which is a zone that can easily be reinforced without changing the overall design. In the case of INC and LMOL maximum stress of 84 MPa and 132 MPa is observed (respectively, in the same location).

The prosthesis was also simulated also under maximum masticatory force without bone ingrowth (second contours in figure 7). As expected, there is a higher concentration of stress surrounding the screws when there is no ingrowth. Additionally, there is also the highest maximum stress in the same location as previously discussed. This situation reached the 190 MPa of Von Mises stress, although it will only take place in the few weeks after implantation where the full load is taken by the screws, so it can be expected to decrease after the bone has grown into the implant. It should be noted that in the situations studied in these sections, the MC is assumed to make contact with the osteotomy platform since this is the situation depicted by the CT-scans.

4.3- Stresses in the fossa component

4.3.1- Contact

In figures 8 and 9, the Von Mises and compressive stress contours are shown for the contact between the MC and the FOSSA_PE. As predicted by contact mechanics, the highest Von Mises stress takes place around 1 mm under the surface of the UHMWPE as seen in figure 9. However, the element size is not fine enough to perfectly locate the point where the highest Von Mises stress takes place (the element edge size would have needed to be around 0.2 mm which would have increased the computational

cost of the simulations to an impractical point). Nevertheless, in figure 11, the analytical solution (calculated with Hertz contact theory) for the stress distribution in both the FOSSA_PE and the MC is displayed. Furthermore, the only task that reaches the yield limit of the UHMWPE is MAX with 45 MPa of compressive stress and 22 MPa of Von Mises stress (through FE method) and 24 MPa and 46 MPa for Von Mises and compressive stress respectively, through Hertz contact theory. For the INC, RMOL, and LMOL the maximum compressive stresses are 23, 40.8 and 35.16 respectively.

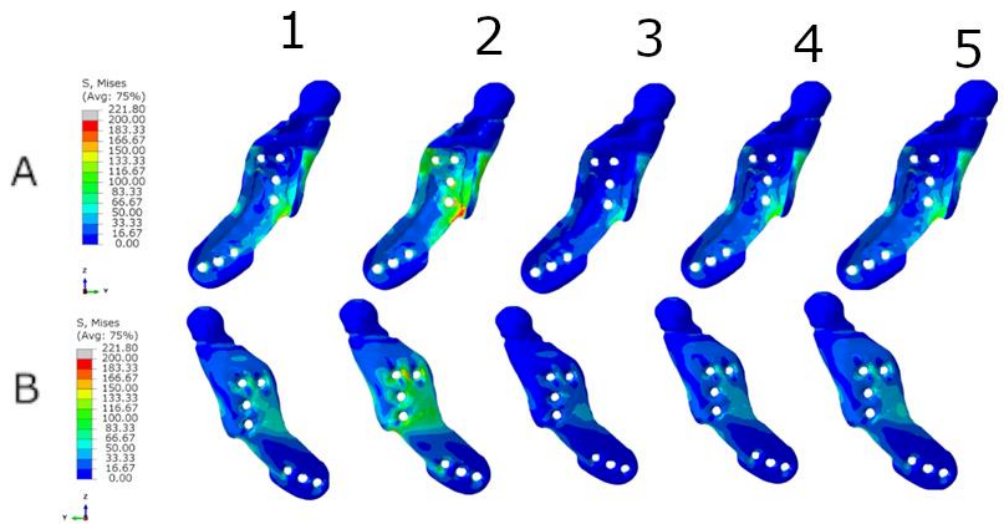

Figure 7: Von Mises stress contours of the mandibular component in the following tasks from left to right: (1) MAX with bone ingrowth, (2) MAX with no ingrowth, (3) INC, (4) RMOL, (5) LMOL. (A) medial view and (B) lateral view

In figure 9, it can be observed how the Von Mises stress is higher in the MC given its much lower Poisson's coefficient (see Table 2). Figure 9 can be compared to figure 10 to obtain the exact stress distribution predicted by Hertz theory. It can be observed how the stress distribution in the MC is better predicted (than in the FOSSA_PE) since the highest Von Mises stress appears around 1 mm under the contact surface.

The FOSSA_TI undergoes lower loading than the FOSSA_PE since the contact surfaces with both the skull and the FOSSA_PE are larger in this case. In addition, the yield strength of the FOSSA_TI is orders of magnitude greater than the FOSSA_PE. Consequently, as seen in figure 11, the highest Von Mises stress this component is

subjected to is 50, 24.5, 45.3 and 39.1 MPa, which is orders of magnitude under the material's yield limit.

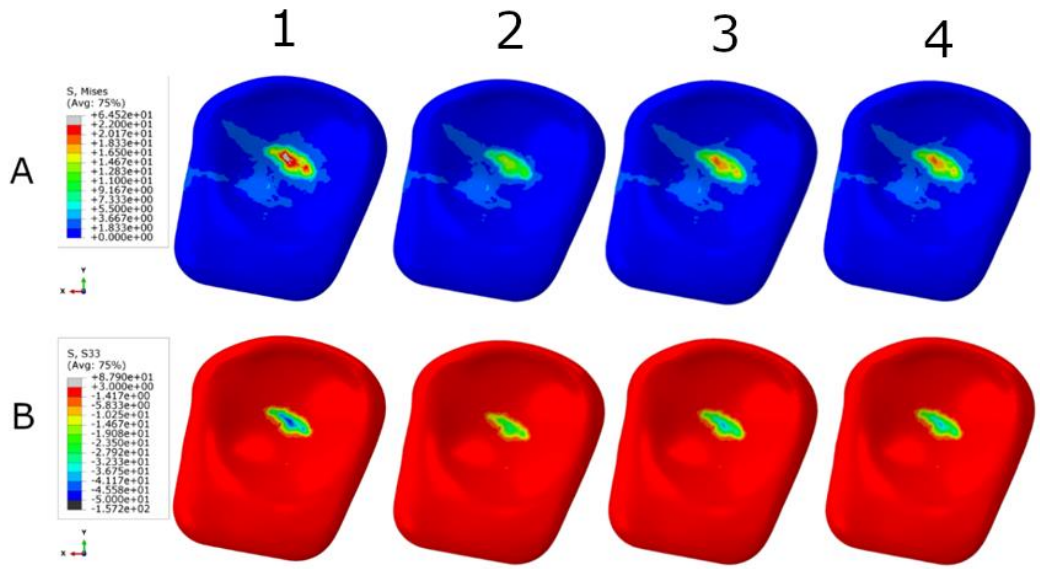

Figure 8: (A) Von Mises and (B) Compressive stress in the fossa component for the 4 tasks. From left to right: MAX (1), INC (2), RMOL (3), LMOL (4).

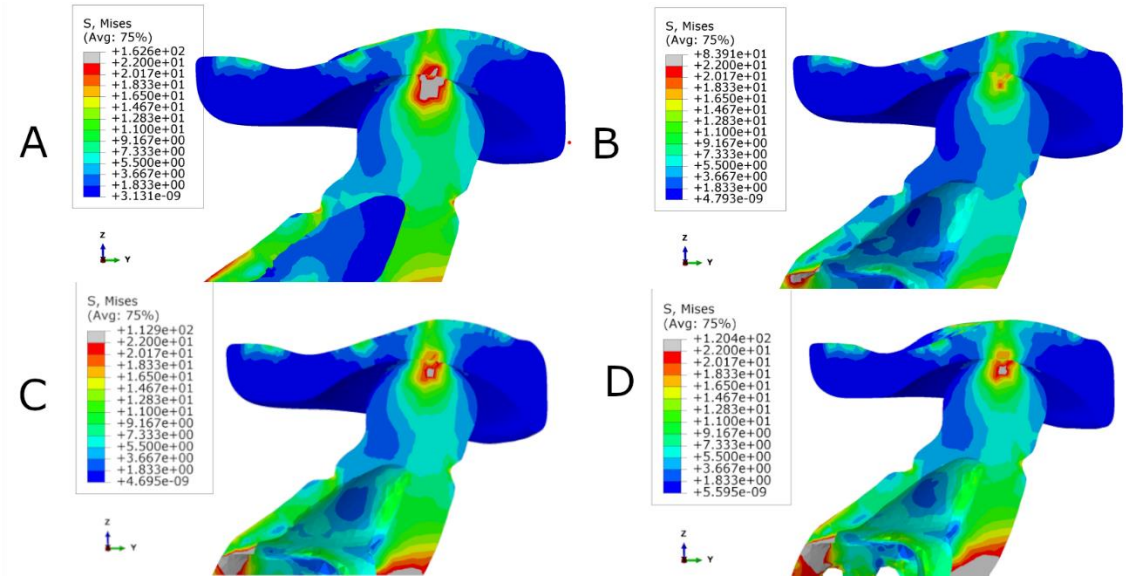

Figure 9: Contact and Von Mises stress in the 4 clenching tasks. MAX (A), INC (B), RMOL (C), LMOL (D)

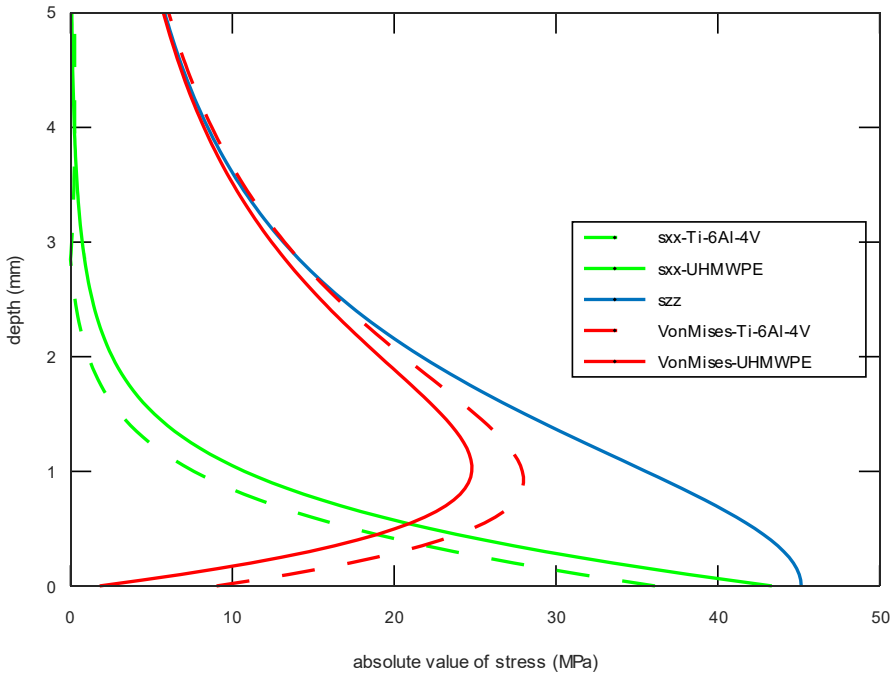

Figure 10: Theoretical solution of the compressive, shear and Von Mises stress below the interface for UHMWPE and Ti-6Al-4V for the MAX task where the load simulated is 350 Newtons

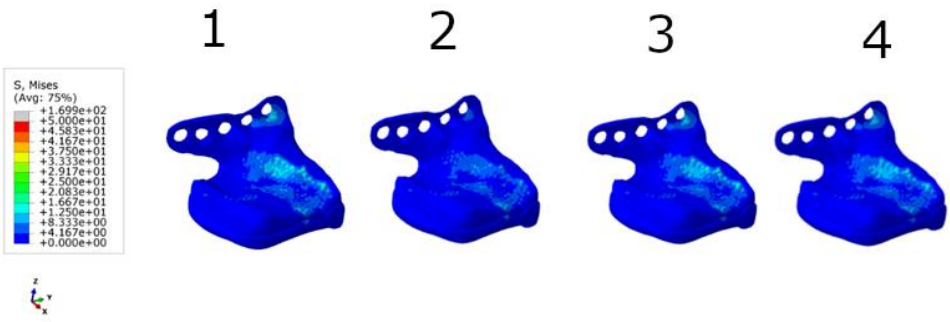

Figure 11: Von Mises stress of the fossa component in the contact side with the skull bone for the 4 clenching tasks. From left to right: MAX (1), INC (2), LMOL (3), RMOL (4).

4.4- Screw Loading

4.4.1- Normal screw configuration

As previously mentioned, in this study, the loads the screws are subjected to will be used to model the overall quality of placement of the screws, and to evaluate the influence of the bone ingrowth into the implant. From the difference in loading visualized in figure 12, it can be confirmed that bone ingrowth will substantially

decrease the loading on the screws. The quality of the placement of the holes can also be evaluated in figure 12 where the division of load can be observed. The first 4 screws bear most of the load leaving the 3 bottom screws almost free of loading.

By assuming pure shear loads on the screws (ignoring the shear load created by the friction with the bone, or any compressive forces) a rough approximation of the maximum Von Mises stress in the 2nd screw can be obtained (shown in equation 1 and 2). This result can be compared with other custom-made prostheses to evaluate the quality of the approximation as well as the load distribution of the screws. This will be discussed further in the next chapter.

$$\sigma_{shear,max}(d = 2mm, pure\ shear\ load) = 79.5MPa$$

Equation 1

$$\sigma_{Von\ Mises,max}(pure\ shear) = \sqrt{3} * \sigma_{shear,max} = 137.83MPa$$

Equation 2

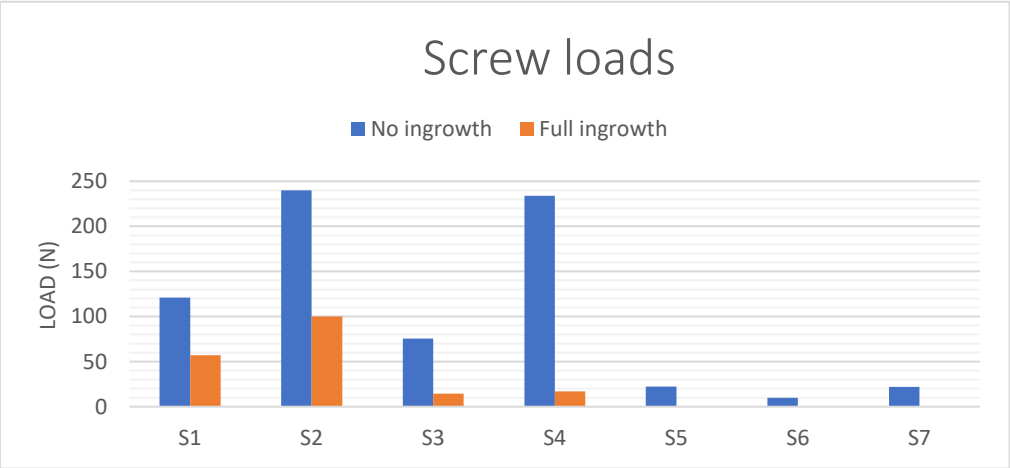

Figure 12: Loads carried by the screws post-operative (blue) and when full bone ingrowth has been achieved (orange)

4.4.2- Other possible screw configurations

In figure 13, the load distribution among the screws is shown when some (or all) of the top 4 are eliminated. In the FULL situation, where all the screws are considered, a noticeable higher load reaching 240 and 234 N can be observed on the 2nd and 4th screws. Given the low loads withstood by the 1st and 3rd screw, the logical next step

that follows is to remove them. Following that premise, a very similar situation is created where the 2nd and 4th loads increase to 283 and 257 N respectively. These two situations provide similar results, although they do not noticeably improve the implant position in relation to the lateral marginal branch of the facial nerve given that the 2nd screw is still positioned.

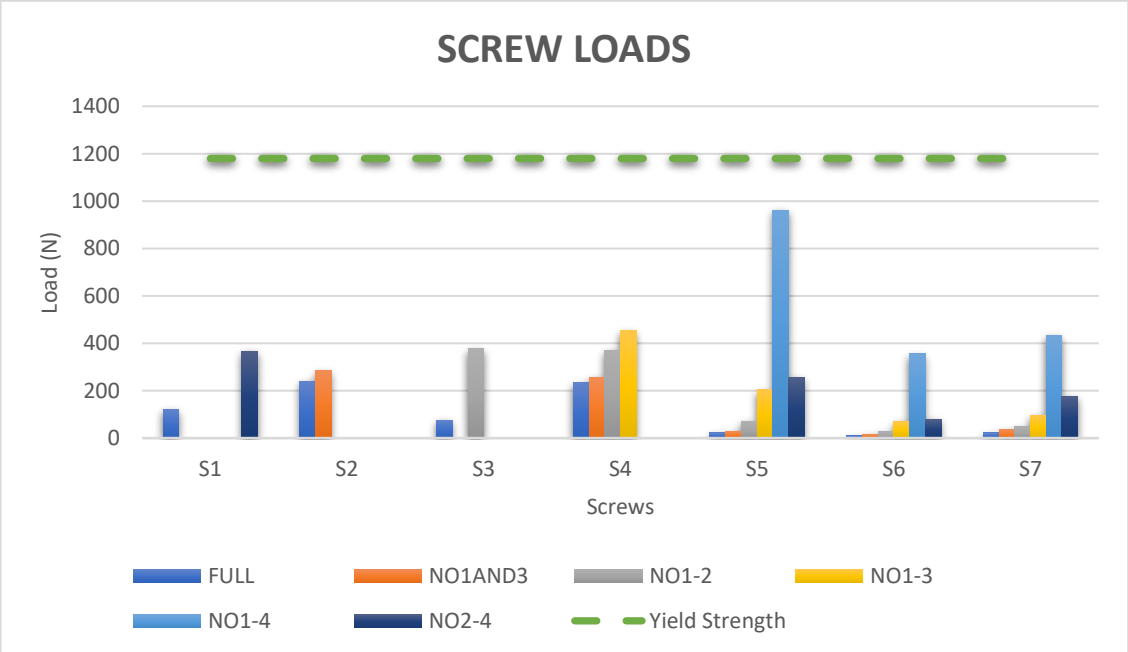

Figure 13: Load distribution among screws for different configurations. The legend reflects the number of screws that were eliminated in the simulation. Numbers in the legend indicate the range of screws that were eliminated from the simulation

When the 2 or 3 top screws are removed, the situation does not vary substantially increasing the maximum load taken by any screw to 371 and 433 N respectively. Additionally, these situations are more interesting given that the screws situated near the lateral marginal branch of the facial nerve are removed. Furthermore, in figure 15 the micromotion experienced by the mandibular component with respect to the bone is shown. The contours are represented in μm and the maximum micromotion displayed is 28 μm. This threshold was chosen according to the most conservative measure found in the literature [17,43].

One last situation is explored where all the top screws are removed. It can be observed in figure 15 how bone ingrowth would most likely not take place in this situation given that most of the implant falls outside of the 28 μm threshold for micromotion.

Furthermore, the load increase experienced by the 5th screw corresponds to a greater than 100% increase than any of the highest load of any of the previous cases.

A highest possible load was calculated in function of the yield strength and the geometry of the screws used (shown in green in figure 13). Given that the actual geometry of the screws is not included in the simulation the maximum load carried by each screw will be used as a failure criterion. The stress state in the screws is assumed to be of pure shear which is a gross simplification. However, a safety factor of 50% is applied to the highest shear load allowed in the screws obtained from this calculation (which means the highest shear load allowed by a single screw is closer to 2400 N rather than 1180 N like it is displayed in figure 13). This safety factor provides a high degree of reliability regarding the stability of this implant as it will be explained in the next section. Furthermore, an error of 0.5 mm was assumed when implanting the mandibular component which means that during loading the implant will not have the support of the bone and all the load will be withstood by the screws which represents a loading scenario considerably worse (regarding the screws and micromotion) than the real one obtained from the CT-scans.

$$\sigma_{Von\ Mises,max}(pure\ shear) = \sqrt{3} * \sigma_{shear,max} = 231.56\ MPa$$

Equation 3

4.5- Micromotion

In figures 14 and 15 the contours for motion with respect to the bone are shown. The upper limit of 28 μm is fixed so no element that shows a higher micromotion will be displayed in the contours. The maximum micromotion observed in the scaffold in the case of removing the top 3 screws (figure 15) is 25 μm the average being 11 μm so it can be considered that osseointegration of the MC would be possible. It should be noted that the simulations run here (figures 12 to 16) did not include bone ingrowth given that the micromotion is only interesting right after surgery.

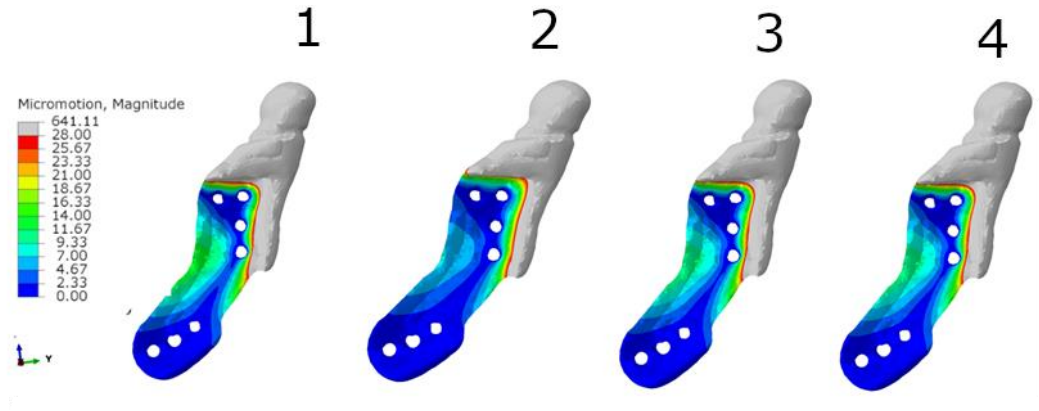

Figure 14: Micromotion (µm) of the mandibular component with respect to the bone. Images are shown for the tasks of MAX (1), INC (2), LMOL (3), RMOL (4).

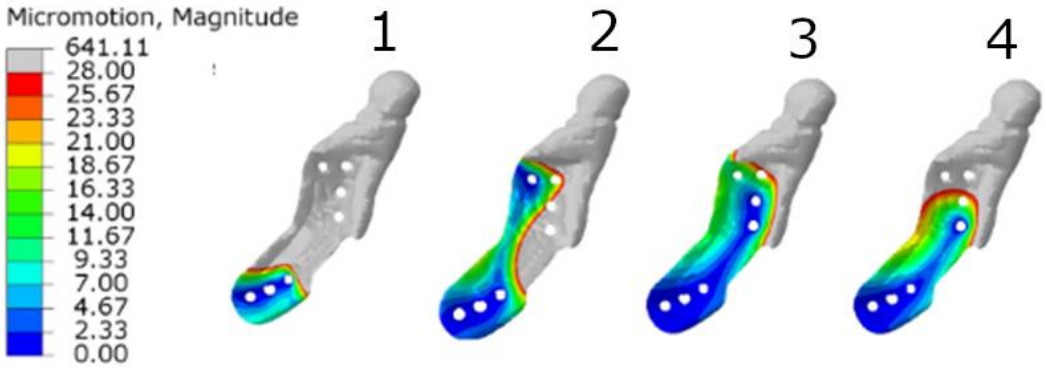

Figure 15: Micromotion (in µm) of 4 cases. Screws 1 to 4 removed (1), screws 2 to 4 removed (2), screws 1 and 2 removed (3), screws 1 to 3 removed (4).

4.6- Load distribution and effect on the healthy side

Another interesting measurement of performance of the TMJ prosthesis is the influence it has over the healthy side. When performing the reconstruction, overload of the healthy disc must be avoided. In figure 16, the difference in load between the right and left side is displayed. It can be noticed how in the healthy model the load is not completely symmetrical.

It is important to recognize how the unilateral clenching tasks see a substantial increase in the loading of both joints. In the healthy model during LMOL and RMOL, the left and right condyles experience a 180 N (when compared to MAX, see Table 4) decrease in loading. In the prosthetic situation, this does not take place and both sides remain heavily loaded during these tasks. Nevertheless, this will not suppose a

problem regarding the failure of the materials, since both situations experience a lower load on both sides than the MAX tasks. For all the values on the condyles loading during the 4 clenching tasks, see Table 4.

The maximum load taken in the diseased model corresponds to 310 N and it takes place in the RMOL task. Surprisingly, this is a decrease from the 330 N of the same task on the same side in the healthy model. Furthermore, this is the only task where there is a decrease in loading from the healthy to the prosthetic model (in the loading of the healthy side).

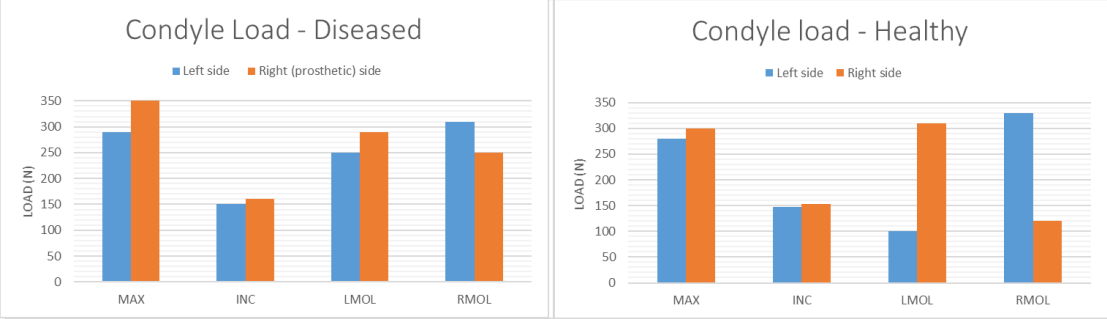

Figure 16: Load distribution in both condyles for the prosthetic and healthy models

Table 4. Values of condyle loads

MODEL	TMJR		Healthy	
	left	right	left	right
MAX	290	350	280	300
INC	150	160	147	153
LMOL	250	290	100	310
RMOL	310	250	330	120

4.7- Strain in the mandible bone

The characteristic strains were analyzed in each of the models. These characteristic strains are given by 4 lines that expand through interesting surfaces (shown in figures 17,18 and 20). Furthermore, the Von Mises (micro)strain is shown, for reasons that

will be expressed in the next chapter. Line 1 expands through the whole mandible bone, from one ramus to another; it will aid in the analysis of the strains in the surface of the mandible bone. As seen in figure 17, the same tendencies are followed by the microstrain pattern in both models. Moreover, there are two spikes of strain in the mandible, one at the cranial side of the ramus where the values for both models are quite similar (637 and 627 με for the healthy model and 588 and 535 με for the prosthetic model). The main difference between the two models resides in the spike in the Von Mises strain that takes place in the caudal side of the ramus (right under the attachment of the superficial head of the masseter muscle). This spike is visible in both figures 17 and 19. In the prosthetic side, it reaches the maximum value of strain of 840 με against the 606 με that take place symmetrically in the healthy model.

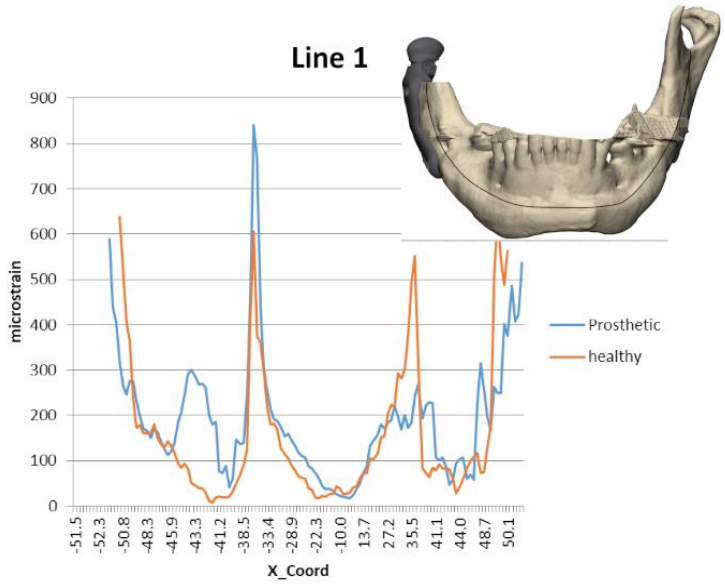

Figure 17: Microstrain (Von Mises) along line 1 for the healthy and the prosthetic model. Keep in mind the differences in geometry observed in figure 5, only the prosthetic model is represented. The Maximum microstrain in the prosthetic model reaches 840 με and 640 με in the healthy model.

In figure 18, lines 2 and 3 provide information on the influence the implant has over the load transfer through the condyle. Here, the healthy side (left) is compared with the prosthetic side (right) of the same model. This approach allows for better evaluation of the results rather than comparing it to the healthy model since the ultimate objective of the implant is to replicate the healthy geometry and the strain profile shape can be expected to remain the same on the healthy side since the

changes introduced after surgery are taking place on the opposite side of the mandible bone. It is observed that the tendencies once again are similar; there appears a spike in principal strain behind the condyle (or behind the implant). This spike reaches a higher value of 1120 με and the healthy side 824 με. The rest of the values for the maximum strain and stress are shown in Table 6.

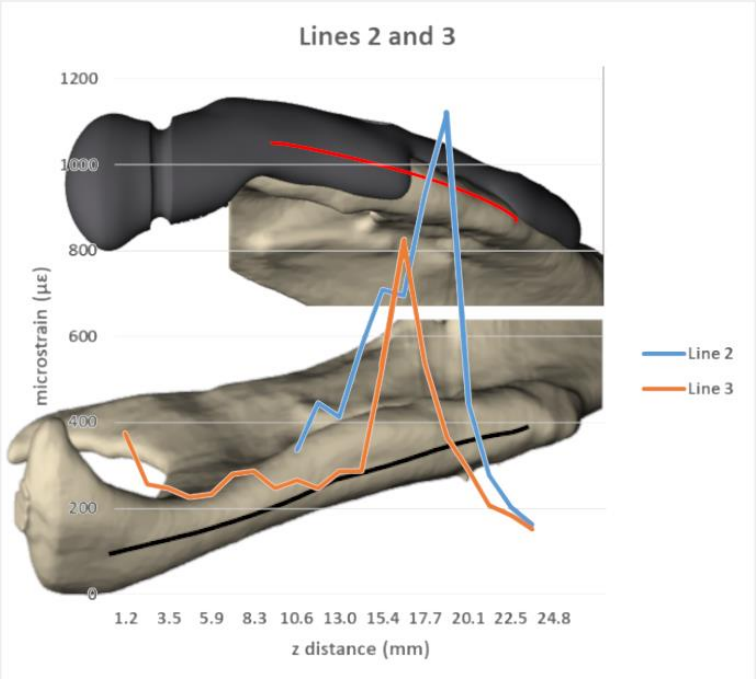

Figure 18: Microstrains (maximum principal) through lines 2 and 3. Both lines present in the prosthetic model. Line 2 reaching a maximum of 1120 με and line 1 824 με.

The contours of microstrain are depicted in figure 19. It is apparent that the maximum strain takes place (in both models) at the caudal side of the coronoid process since this is where the temporal muscle attaches, which was shown (in table 3) this is the main muscles of mastication. These strains correspond to the values of 4700 με and 3100 με in the prosthetic and healthy model respectively (see table 16).

4.7.1- Comparison with healthy model – stress shielding

Stress shielding must be avoided in order to preserve the healthy bone that is left in the mandible. To evaluate stress shielding, the data is extracted from the surface that establishes contact with the scaffold and solid implant. As depicted in figure 20, line 4 is drawn in between the screws underneath the implant (on the surface of the bone). The strain data out of that line is depicted in figure 20 for the MAX task and for both

situations: bone ingrowth and no bone ingrowth. As expected, the strain is lower when there is no bone ingrowth since all the load is taken by the screws (the line does not go through any screw hole). However, this strain does not go under the threshold of 100 με which is considered the minimum value for bone resorption to take place. Furthermore, outside of the scaffold (23 mm and over in figure 20), the strain profile is the same in both situations given that the loading is taken by the bottom three screws in both cases.

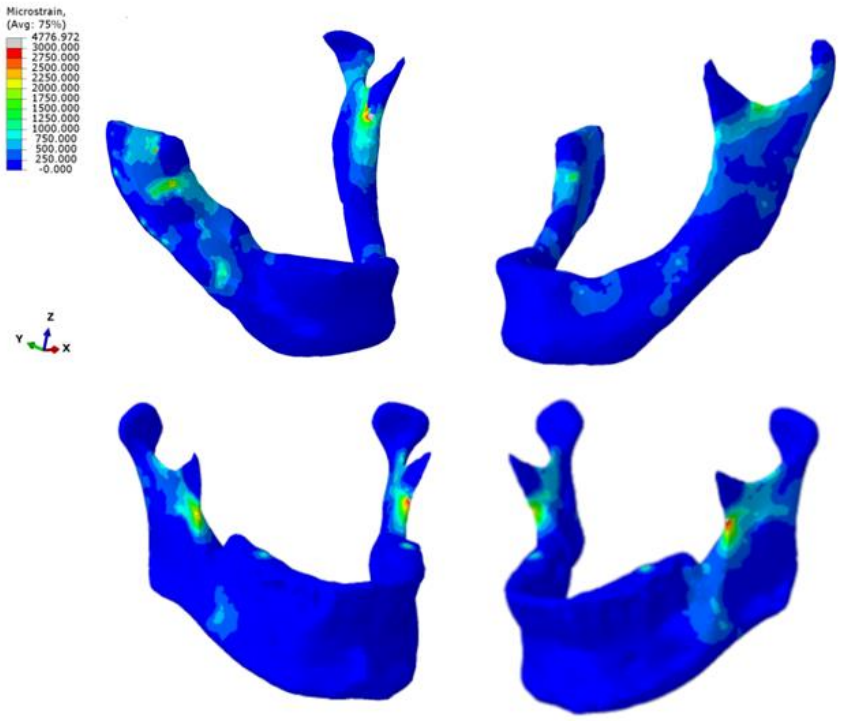

Figure 19: Microstrains in the posterior side of the condyle for both healthy and diseased models

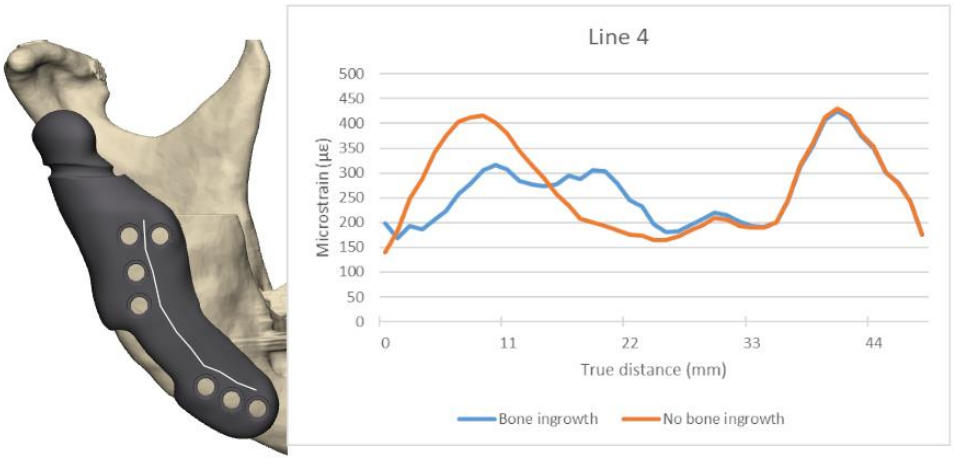

Figure 20: Microstrains through line 4 situated under the implant on the surface of the bone. Maximum and minimum values reached both by the case with no bone ingrowth with values of 430 and 169 με respectively.

4.8- Dynamic simulation

As previously mentioned the 4D CT-scans record the patient performing a full mastication cycle which reaches 18 mm of mouth opening (distance between the incisor teeth). In order to simplify the results, the data obtained for 3 interesting mouth openings are displayed in this chapter. The distance for each of them is 4mm, 9mm and full opening (18mm). In figure 21, the stress contours for the prosthesis' components and the strain contours for the mandible is shown for each of these 3 jaw positions. As shown in figure 22, the load taken by the prosthesis decreases with the opening of the jaw. Given this result, it can be understood how the stresses and strains displayed in the components shown in figure 21 decrease with the mouth opening. Furthermore, the maximum stresses displayed for each component are 143 MPa for the MC with 8 mm opening, 18 MPa for the FOSSA_PE with 18 mm opening, 45 MPa for the FOSSA_TI with 5 mm opening, 2600 με for the mandible at full opening (in the right ramus not considering the attachment of the temporalis muscle) and 2476 με for the left condyle for 18 mm opening. More results are shown in Table 6.

Notice how, in figure 22, the load in the healthy condyle increases with opening, reaching the highest load of the whole study for the left condyle: 432 N. In table 5, the maximum, minimum and average values of strain through the lines (previously described) is displayed. As expected, the strain through line 3 (which travels along the back of the left condyle) increases with the opening of the mouth given that the

load also increases from 369 to 462 με. Furthermore, the strains in the prosthetic condyle decrease with the opening for the same reason. Further discussion about the strains in the bone will take place in the next chapter.

Since the load on the right side (implant) is reduced when the mouth opens (see figure 21) the loads on the screws decrease compared to the loads presented in figure 12. Furthermore, in the dynamic simulation, the support of the bone on the implant was considered, thus decreasing the load taken by the screws substantially.

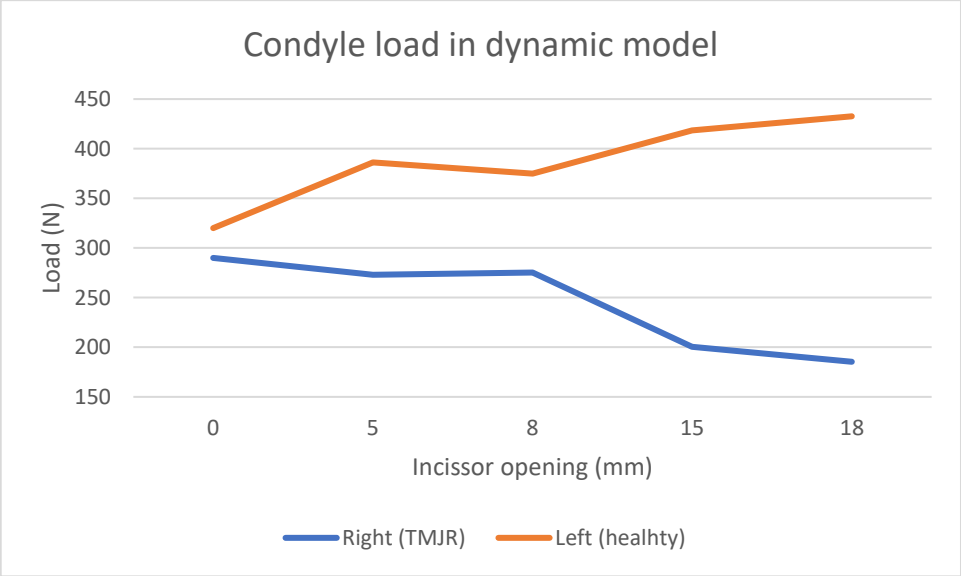

Figure 21: Load transmitted by each condyle for each mouth opening position.

Table 5: Maximum, minimum and average microstrain values through lines 1,3 and 4 in the dynamic model.

	Incisor opening (mm)	MAX (με)	MIN(με)	AVERAGE(με)
LINE 3	18	1007.4	203.2	462.0
	8	883.3	195.2	382.3
	5	977.0	177.6	415.2
	0	848.6	179.1	369.4
LINE4	18	241.6	71.6	168.8
	8	286.6	112.5	206.9
	5	314.0	126.7	219.9
	0	385.51	165.5	266.6
LINE1	18	1494.2	0	313.0
	8	1501.8	0	298.1
	5	1658.4	0	299.1
	0	1590.0	0	319.9

Table 6: maximum stress and strain values for the prosthesis components and mandibular bone during four clenching tasks and dynamic simulation. In the dynamic model, the attachment of the temporalis muscle is not considering as maximum strain for reasons shown in the next chapter.

Model	Tasks	MAX	INC	LMOL	RMOL	Dynamic	Opening
		Von Mises stress in MPa (strain in με)					(only for dynamic)
TMJR	**MC**	169 (1600)	84.5 (800)	143.65 (1360)	179.14 (1696)	143 (1360)	8mm
	FOSSA_PE	22 (19000)	11 (9500)	18.7 (16150)	23.32 (20140)	18 (30000)	18mm
	FOSSA_TI	50 (400)	25 (200	42.5 (340)	53 (424)	45 (360)	5mm
	Mandible	80 (4700)	40 (2350)	72 (4230)	62.4 (3670)	50 (2600)	18mm
	Left Condyle	15 (800)	7.5 (400)	13.5 (720)	11.7 (624)	24 (1476)	18mm
Healthy	**Right Condyle**	10 (600	5 (300)	8.5 (510)	10.6 (636)		
	Left Condyle	12 (700)	6 (350)	10.8 (630)	9.36 (546)		

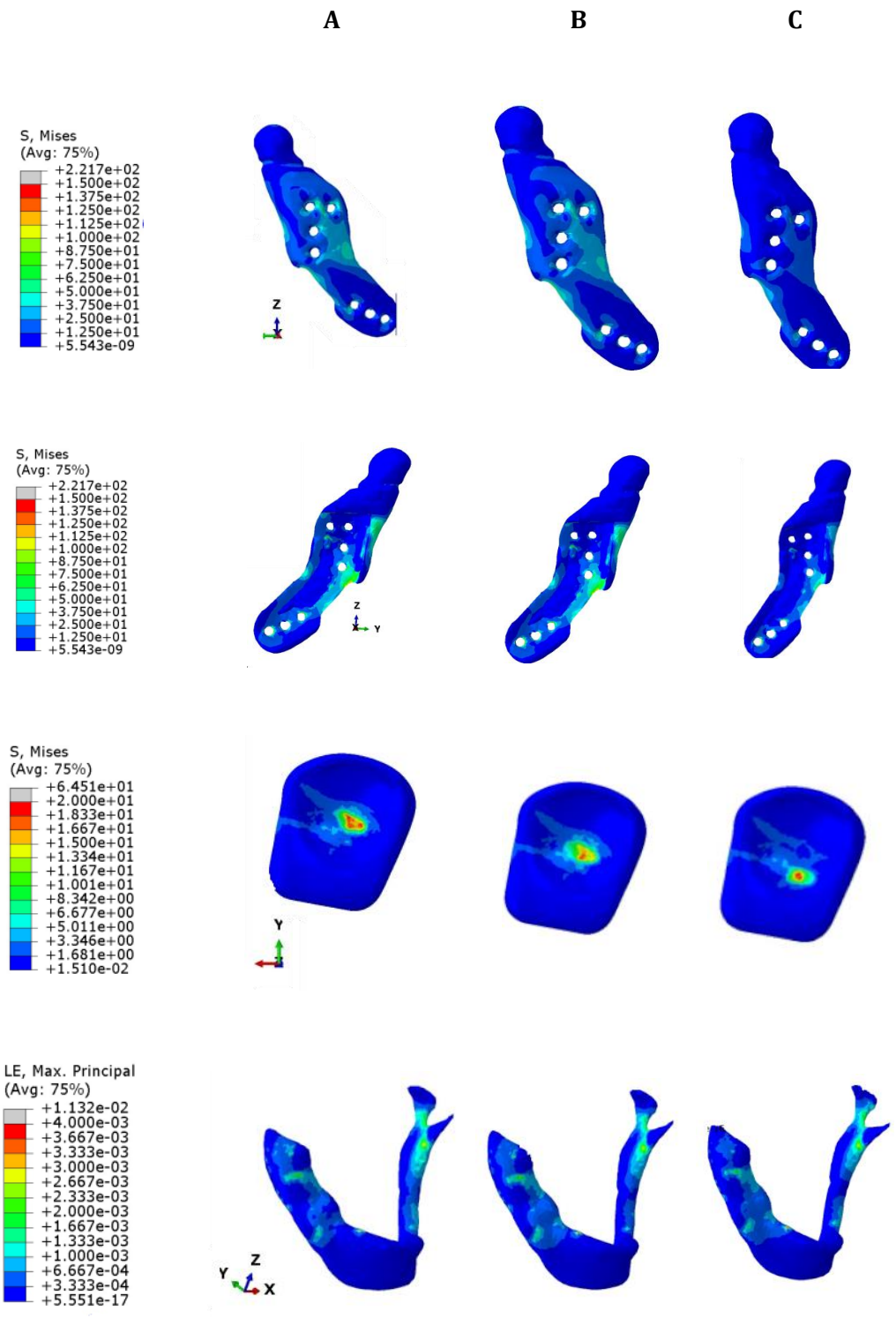

Figure 22: Stress and strain contours for the dynamic model with three mouth opening positions. A: 5mm, B: 9mm, C:18mm

4.9- Conclusions

In this chapter, the loading scenarios taking place during the 4 clenching tasks and the dynamic model are displayed. The fact that the condyle and, in general, the Ti-6Al-4V components are subjected to stress much below their yield strength has become apparent. Furthermore, the main structures working near their capabilities have been shown to be the FOSSA_PE and the healthy condyle when performing maximum muscle activation (MAX) with the mouth fully open. In the latter case has been shown how the implementation of the 4D CT data provides insightful information that would not have been captured with the static analysis. Additionally, the analysis of strains throughout the mandible bone has provided useful data that will be further analyzed in the next chapter to evaluate stress shielding, bone resorption and bone hypertrophy.

Chapter 5 - Discussion

The main objective of this study was to evaluate the performance of the CADskills TMJ prosthesis "parametron classico". This evaluation is made by analyzing the influence that the prosthesis has on the mandible behavior and the loads the materials will be subjected to during physiological loading. The following chapter provides an analysis of the results obtained from the FE model and a discussion on the limitation of the model.

5.1- The Finite Element model

The FEM is a numerical approximation of the behavior of the materials involved in the simulation. Several approximations are made in order to be able to construct a model of the whole mandible, such as: discretization of the continuum into small elements (tetrahedrons in this case), linear elastic materials, fixed boundary conditions in the skull, etc. Even though experimental validation of the FE model has not been done for this study, several FE models have been previously validated in vivo [7]. Furthermore, FEA has been used in biomechanics to simulate the interaction between biological structures and artificial materials for many types of orthopedic devices providing great results [44,45], and also (although less common) with TMJ prosthesis [5,6,9,12,19,42,46].

During the formulation of the FE model several assumptions were made regarding the materials. Firstly, the bone was assumed to be isotropic and linear elastic. This is a limitation of this study that will be discussed further in this chapter, however, under the circumstances, the bone is loaded (see Table 6) it is an acceptable assumption that bone will present an elastic behavior. Same could be said about the rest of the materials. As can be seen in Table 6 none of the prosthesis' materials are loaded further than the elastic yield limit. This can be said of every material except the UHMWPE which reaches the yield strength limit in the contact site with the MC for the MAX task (see figure 9).

To analyze the loading of the different materials, the Von Mises stress was mostly used, especially when the stress contours are displayed. The stress contours perform outstandingly in the task of conveying the information that is needed in this case (the loading situations of different materials) even though this information is analyzed in

a qualitative manner since exact values are not displayed in this type of representation. Furthermore, it allows for the visualization of almost every single point of the 3D geometry. However, since stress is fully represented by a second order tensor, the simplification to a single point scalar (which is done when representing the stress contours) simplifies substantially the information captured by the stress tensor. This simplification to a single scalar value was (in most cases) made for the Von Mises stress given its widespread use in previous research, and also because the maximum distortion energy criterion was used to diagnose the failure of the materials. The exact same thing can be said when treating the Von Mises strain for bone. In this case, it is assumed bone fracture (or hypertrophy, or resorption) will take place when a given threshold for the distortion strain is surpassed.

5.1.1- MC and FOSSA_TI

It is assumed that Ti-6Al-4V will experience plastic deformation when the Von Mises stress reaches 1301 MPa. In figures 7 and 11, and Table 6, it can be observed the requirements of this material fall under its capabilities when the maximum stress it is subjected to through all tasks is 190 MPa. Furthermore, the load on the MC will decrease as long as bone grows into the scaffold.

5.1.2- Contact FOSSA_PE with MC

UHMWPE has numerous advantages when it comes to implants, like high wear resistance, high stiffness, high yield strength and a low friction coefficient with the MC (compared to other polymers) [47]. However, in the case being studied the polymer is under circumstances that may lead to permanent deformation due to high loads transmitted between the MC and the FOSSA_PE. Furthermore, high stresses, in this interface, have already been seen in previous research, especially when dealing with custom-made prosthesis [5,12]. Because this stress is close to the yield strength of the UHMWPE (as displayed in figure 8), it is of high importance that it is accurately modeled in the FE model in order to have a correct assessment of the working conditions of the prosthesis. Abaqus has several options to model contacts depending on the stiffness of the materials involved, the geometries, the expected motion between them, the definition of the geometry, etc. It is shown in figure 7 and 8, how the Von Mises stress reaches its yield limit with the MAX task near the surface of contact. However, when the situation is analyzed further, it can be observed in figure

9 how the Von Mises stress reaches its maximum at around 1 mm, away from the contact surface due to the small contact point between the components. Given the load in the right fossa, observed in figure 16, the analytical solution with the equations of contact mechanics yields the Von Mises stress of 24 MPa (displayed in figure 10). However, when this calculation was performed, the contact was assumed to be between a perfect sphere and cup taking the lowest diameter of the head of the MC. The real results will yield lower stress since the head of the MC component is not a sphere but resembles more an ellipsoid. Thus, it can be concluded that the contact simulation performed in Abaqus yields acceptable approximate results of the stresses the UHMWPE is subjected to. Furthermore, when the compressive stresses are considered (figure 8 and 10) the same conclusion can be derived. The approximation of the Von Mises and compressive stress made by Abaqus is highly accurate. However, it is not possible to estimate this accuracy exactly since the analytical solution has also been obtained through some geometrical assumptions. Overall, it can be concluded that the UHMWPE performs close to its yield limit during the MAX task. Furthermore, the fact that the MAX task corresponds to an idealized situation of full muscle activation should be kept in mind. No sign of this situation taking place has been shown in literature [17,34]. So even though, the UHMWPE is performing close to its yield strength, in the figures 8, 9 and 22 is shown that for the "real" situations (LMOL, RMOL, and INC) the yield strength limit (22 MPa) is not surpassed

In conclusion, the contact results between the FOSSA_PE and the MC have been validated and are in agreement with previous research on custom-made TMJR [5]. The fact such high Von Mises stress is reached might produce abrasion in the FOSSA_PE after long term used. However, maximum activation of every muscle does not take place in the literature and that was the only case where such high stress appeared on the UHMWPE.

5.1.3- Screws

The screws are an important component of the prosthesis and for that reason have been thoroughly analyzed in previous investigations regarding TMJR [1,5,6,12,14,17,19]. As previously mentioned, in this study, the 3D geometry of the screws is not modeled but the mechanical influence of the screws in the prosthesis and the bone is incorporated into the FE model. Furthermore, the loads taken by each

screw are used to analyze the load distribution shown in figure 12. These loads are used to compare the distribution with other custom-made prostheses in literature. As it is displayed in figure 12 the 2nd and 4th screw take most of the load. This is expected given that the higher the screws are placed the majority of the load in all TMJ prostheses [5,6,14,19,46]. When comparing the results with other custom-made prosthesis like the one developed by [6] or [17], the prosthesis from CADskills performs similarly. A better distribution of loads could be achieved by placing the first screw in a higher position, so it would share some of the load with the second screw (which is the one that is absorbing the highest load of 435 N). Another improvement could be done by placing the fifth screw closer to the fourth so this load could also be shared and that way decreasing the peaks in screw load that take place in the second and fourth screw.

Given the proximity of the marginal mandibular branch of the facial nerve to the top screws in the prosthesis it might be useful to remove the top three screws. Simulations where conducted removing different combinations of the screws of the MC. The loading that resulted from the MAX task by each combination is displayed in figure 13. In this situation, with the pure shear load simplification, the maximum stress obtained is 231.56 MPa, which is less than 20% the yield limit of Ti-6Al-4V. It can be concluded the removal of the top three screws would not produce failure of the screws but further FE research with the correct modeling of the screw geometry or experimental research should be conducted to prove this.

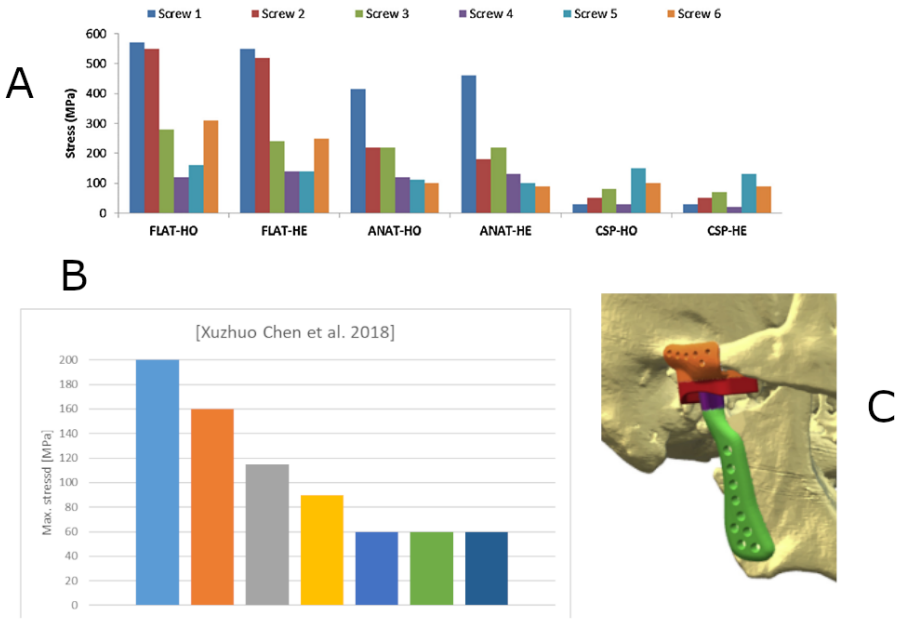

Figure 23: Max Von Mises stress in the prosthesis developed by [6] (A) and the custom-made prosthesis developed by [6] (B and C). FLAT/ANAT=Flat contact surface/Anatomical fit between the mandibular component and the mandibular ramus (both Christensen prosthesis); HO/HE=Homogeneous/heterogeneous bone modeling; CSP=Custom-made condylar support prosthesis

5.2- Osseointegration

Micromotion is a fundamental parameter used to evaluate the performance of the prosthesis. Excessive micromotion between the MC and the bone not only causes instability of the prosthesis which might lead to loosening and thus failure of the implant. Furthermore, bone ingrowth is strongly desired since the results shown in the previous section display lower stress shielding, lower loads carried by the screws and it would provide higher stability of the implant. Furthermore, osseointegration and stability are evaluated through the concept of micromotion [14,19,38,40,41,48]. If the implant is displaced above a certain threshold with regards to the bone, ingrowth will not take place. There are discrepancies on the value of this threshold. Some authors suggest that 40 μm is the highest value for osseointegration to take place [40,41,43]. However, in this study, the threshold use was 28 μm which is the most conservative found in literature [17,43].

It is observed in figure 14 that osseointegration will take place in the scaffold of the MC given that, for all tasks (with all 7 screws), the micromotions were well under 28 μm. Furthermore, these results were obtained assuming a 0.5 mm placement error during surgery, which would not allow for the MC component to make contact with the osteotomy platform. This constitutes an unreal situation since the CT scans show perfect contact between the implant and the bone. The same premise was followed to obtain the results when the top four screws were not present. The case for removing the top three screws (which is the most interesting one as previously mentioned) gives satisfactory results since the complete scaffold experiences less than 28 μm of motion during the MAX task.

5.3- Influence on the mandible bone and opposite side

The TMJ is the only biarticular joint in the body. Consequently, this implies when one side of the joint is modified that this will have results on the opposite side, and they ought to be limited for this situation. Only a few studies have evaluated the kinematics of contralateral natural joints in patients with unilateral total joint reconstruction [5,9,48]. Perez et al. [49] conducted research on the consequences of increase loading whether patients, that had undergone TMJ reconstruction, suffered any adverse effects on the healthy articular disc. They did not find signs of pain or discomfort in the patients, however, others have shown that long term overload of the joint will cause failure of the disc [15]. In this case, a 3.6% increase in the load of the contralateral joint is observed with the MAX task, which is also the one producing the highest loads (in the contralateral side). This result concurs with previous research where custom-made prosthesis were used [3,5,8]. The little increase in contralateral joint loading is attributed to the fossa component's geometry which has been manufactured to mimic the motion of the healthy condyle [1].

When analyzing the dynamic model an increase in contralateral loading can be observed with increasing incisor opening. This result does not reflect the real situation since the muscular loads were not modeled as a reaction of the loads in the teeth and the length of the muscles. Furthermore, there is no information regarding the muscular activation after TMJ reconstruction. Previous models have been developed analyzing different mouth apertures after TMJ replacement (although the

source of the instances positions is unknown). Further discussion on this topic can be found in the limitations section.

5.3.1- Strain distribution

The strains produced in the mandible after the prosthesis has been implanted provide some insights into the influence the reconstruction has on the bone. Furthermore, the Von Mises strain was obtained since, as previously mentioned, it conveys the most amount of information regarding bone hypertrophy. Furthermore, it is commonly used in research [5,7,17] so it can be used for comparison. When the healthy and prosthetic models' strains through line 1 are compared, some similarities are found. In the healthy model, the strain distribution is quite symmetrical, as expected. However, there are slight differences in the spikes encountered in the side of the implant. According to previous research, there are two spikes on each side of the mandible, one corresponding to the end of the condyle and load transferred to the ramus and another one after the attachment of the superficial masseter muscle. As shown by the strain through line 1, the spike due to the masseter muscle is intensified given that re-insertion of only part of the muscle is considered, thus increasing the loading in that surface. Finally, the strain distribution in the mandible is not greatly influenced which can also be observed in the strain through lines 2 and 3 where there is a slight increase in strain when the load is transferred from the MC to the bone. However, it is far from causing any damage to the bone.

Furthermore, strain evaluations also provided useful information to analyze stress shielding. Line 1 travels through the area most influenced by the implant and shows how the strain never goes under 100 με which is considered to stimulate bone resorption [50]. Furthermore, the maximum strain found in the bone during static clenching takes place in the condyle as expected, but it is far lower than the considered threshold for bone hypertrophy (4000 με [50]). In the MAX task, however, the microstrain is higher than 4000 με. This takes place in the attachment of the temporal muscle which is always a source of high loads. As in previous research, this is not considered a failure, given that it also takes place in healthy individuals [19].

5.4- Limitations

This study is based on a FE model of a set of materials and loading conditions. As any mathematical modeling of a physiological process, there are some limitations to the

study. Firstly, the bone has been considered elastic and isotropic, hence the composite behavior of bone has not been considered. Even though this assumption has been made numerous times in previous research with TMJ prostheses [9,11,12,17] and has provided very similar results when compared to the simulation considering the heterogeneity (cortical and trabecular) nature of the mandibular bone [6].

The 3D geometry of the screws is not modeled only their mechanical influence on the fixation of the implant to the mandibular bone. Consequently, this does not allow for accurate stress predictions on the screws.

The muscle forces and directions are not directly measured in the patients' where the prosthesis is implanted but were obtained from literature. Even though the simulated tasks here correspond to the highest loading scenarios observed in the literature, and that there is quite a consensus in literature on maximum masticatory forces (even accounting for differences among humans) [7,34], it would be helpful if these values and directions could be validated by the actual patient. Furthermore, the results of the dynamic simulation consider muscle forces from literature and patient-specific geometries taken from the CT scan. Thus, the values of the directions are varied in this simulation and that may be a source of inaccuracies in the results. Additionally, in the dynamic model, the change in length, and consequently change in load) of the muscles is not considered, which produces higher stresses and strains in the results than there would actually be. Moreover, the assumption that the masticatory forces will be symmetrical and equal to healthy individuals, as in pathological cases, is most likely wrong.

As previously mentioned, experimental validation is not performed in this particular FE model. Furthermore, failure by fatigue due to cyclical loading is not considered. Further testing should be made (especially regarding the UHMWPE) to evaluate the situation of the implant's materials through cyclic loading.

Another important limitation is the lack of modeling of the non-linearity and anisotropy of the mandibular disc in the healthy side. It is assumed throughout the study that the likelihood of damage of the articular disc increases proportionally to the increase in load of the healthy condyle. This linear relationship has been shown to be wrong, given the viscoelasticity of the disc. However, it has been shown that the

shear stress is the cause of damage to the disc [15] and this stress that has been shown to increase at a lower rate than the compressive loading in the condyle [11].

Only one implant has been evaluated (and in one patient). It is not expected that the behavior of the prosthesis will change radically for other patients since it is custom-made for each patient. However, further studies should be done to confirm the results obtained here and to evaluate in the situations in different patients with different bone geometries.

Chapter 6 - Conclusions

The main objective of this thesis project was to evaluate the performance of the TMJ prosthesis "Parametro Classico" manufactured by CADskills. This prosthesis has similar performance to other custom-made prosthesis in the market. However, in this study more parameters have been studied than any other published research on the topic, so it gives form to a comprehensive analysis of the influence the implant has on the jaw mechanics.

It has been proven that this implant will promote osseointegration under any physiological loading, which will reduce the amount of stress shielding that would take place in the diseased ramus. Furthermore, osseointegration has been shown to take place given that the micromotion is under the most conservative threshold encountered for bone ingrowth into metallic scaffolds. Additionally, these results were obtained assuming a slight misalignment during surgery which would remove the support of the cranial surface of the ramus on the implant.

The components find themselves considerably under yield conditions except for the UHMWPE. Further tests should be ran in order to determine the long term loading of the material and ensure lack of wear.

The mandible bone sees itself mostly unaffected by the implantation of the prosthesis, except where it takes over (superficial masseter) muscle attachment space where it will spike up the strains on the bone since the same force is modeled under a smaller surface area. The ramus where the implant is located will encounter slightly higher loads than the healthy condyle but always under manageable ranges.

The dynamic simulation provides important insights regarding the healthy side. Given that 4D data has not been around for a long time, no study has been published making use of this type of technology. When physiological loading is combined with the 4D data, a slight increase on the healthy side and a substantial compression strain increase on the healthy condyle is encountered. Considering the simulated loading in this study will not take place since full activation of muscles cannot be reached at mouth openings of 18 mm, these results provide only an insight on the influence of the prosthesis on the movement and loading.

No damage is predicted to take place on the healthy articular disc since it has been shown to be able to withstand substantial loads, increases after total TMJ reconstruction without experiencing pain or discomfort [49]. Furthermore, for small mouth openings, the TMJ has shown to be of very little influence on the healthy side.

Even though the exact geometry of the screws has not been modeled, the loads they are subjected to are expected to be substantially under the yield limit of the Ti-6Al-4V. It has also been shown how the removal of the top three screws will slightly increase the maximum stress on the screws, but it is expected to not surpass the yield limit of the Ti-alloy.

Chapter 7 - Future Work

Several limitations have been found for this thesis project. Some of them can be solved on a short-term basis adjusting the FE model by adding some features.

The most relevant one is related to the muscle forces and boundary conditions, since they have been shown to noticeably influence the results of the simulations [33]. If possible, they should be measured in a patient that has undergone total TMJ reconstruction, since there is no data available on the activation of the masticatory muscles after such intervention. Furthermore, there is only data on the maximum muscle activation for certain tooth clenching tasks which is useful for the static model. However, for different mouth openings there is lack of knowledge on the forces exerted by the muscles. This could be solved by implementing a muscle model (e.g. Hill-type muscle activation model [15,28]).

The healthy model was a useful support through the process, allowing comparisons with the prosthetic model. However, it was obvious that the geometries differed substantially which undoubtedly taints the results (and the comparisons). This could be solved by interactively "regenerating" the diseased condyle with the geometry from the healthy condyle of the same patient. This approach would provide a theoretically exact copy of the healthy jaw of the diseased patient. Thus, it would assure any differences obtained between the models would have arisen due to the presence of the implant.

As mentioned in the limitations, the heterogeneous aspect of bone was not considered in this study and it would provide an interesting added value to the research since it would provide more accurate approximations of the strains suffered by the bone. The bone density can be approximated by the HU units of the CT scans which are already available.

The articular disc's geometry or behavior has not been modeled and it is the main component influenced by the prosthesis. Given its viscoelastic properties, it is challenging to predict the influence that the load increase (which has been shown to take place for big mouth openings during maximum activation) will have on the actual disc. There are viscoelastic models for the disc available in the literature that could be implemented into the existing FE model. Furthermore, there is no need to obtain

imaging data to obtain the exact geometry of the disc since there are simpler approaches that have been shown to work well [1,11,15]. The space between the condyle and the fossa is filled with a material with these viscoelastic characteristics.

As any FE model, this model needs experimental validation, even though very similar models of the jaw have been experimentally validated [7]. It is especially interesting to validate the results obtained in the FOSSA_PE since it is predicted to be under stresses near its elastic yield limit. Furthermore, experimental trials have been conducted in sheep with successful results. However, sheep rarely perform a full activation of their masticatory muscles (these loads would anyway be different from humans), and given that sheep are herbivores their diet consists on softer foods than humans [32]. Consequently, it can be expected that the situations the materials of the prosthesis will undergo when implanted in sheep will be less extreme than in humans.

The load on the healthy side has been shown to increase with mouth openings. If we assume this does not take place in a healthy model (hypothesis that needs to be proven by creating a 4D FE model of a healthy patient), it manifests a possible improvement of the design of the FOSSA_PE. Through the evaluation of the mechanics of the healthy model, the design of the FOSSA_PE can be optimized to minimize the load on the contralateral joint.

Bibliography

[1] Ramos AM, Mesnard M. The stock alloplastic temporomandibular joint implant can influence the behavior of the opposite native joint: A numerical study. J Cranio-Maxillofacial Surg 2015;43:1384–91. doi:10.1016/j.jcms.2015.06.042.

[2] Wolford LM, Dingwerth DJ, Talwar RM, Pitta MC. Comparison of 2 temporomandibular joint total joint prosthesis systems. J Oral Maxillofac Surg 2003;61:685–90. doi:10.1053/joms.2003.50112.

[3] Rodrigues YL, Mathew MT, Mercuri LG, da Silva JSP, Henriques B, Souza JCM. Biomechanical simulation of temporomandibular joint replacement (TMJR) devices: a scoping review of the finite element method. Int J Oral Maxillofac Surg 2018;47:1032–42. doi:10.1016/j.ijom.2018.02.005.

[4] N.Kent J. An important lesson about biomaterials in the TMJ. J Oral Maxillofac Surg 1991;49:442–3.

[5] Chen X, Wang Y, Mao Y, Zhou Z, Zheng J, Zhen J, et al. Biomechanical evaluation of Chinese customized three-dimensionally printed total temporomandibular joint prostheses: A finite element analysis. J Cranio-Maxillofacial Surg 2018;46:1561–8. doi:10.1016/j.jcms.2018.06.018.

[6] Abel EW, Hilgers A, McLoughlin PM. Finite element analysis of a condylar support prosthesis to replace the temporomandibular joint. Br J Oral Maxillofac Surg 2015;53:352–7. doi:10.1016/j.bjoms.2015.01.016.

[7] Mesnard M, Ramos A, Ballu A, Morlier J, Cid M, Simoes JA. Biomechanical analysis comparing natural and alloplastic temporomandibular joint replacement using a finite element model. J Oral Maxillofac Surg 2011;69:1008–17. doi:10.1016/j.joms.2010.02.019.

[8] Ramos A, Mesnard M. Comparison of load transfers in TMJ replacement using a standard and a custom-made temporal component. J Cranio-Maxillofacial Surg 2014;42:1766–72. doi:10.1016/j.jcms.2014.06.012.

[9] Bekcioglu B, Bulut E, Bas B. The Effects of Unilateral Alloplastic Temporomandibular Joint Replacement on the Opposite-Side Natural Joint: A Finite-Element Analysis. J Oral Maxillofac Surg 2017;75:2316–22. doi:10.1016/j.joms.2017.05.017.

[10] Voiner J, Yu J, Deitrich P, Chafin C, Giannakopoulos H. Analysis of mandibular motion following unilateral and bilateral alloplastic TMJ reconstruction. Int J Oral Maxillofac Surg 2011;40:569–71. doi:10.1016/j.ijom.2011.01.010.

[11] Eijden JHK and TMGJ van. Consequences of Viscoelastic Behavior in the Human. J Dent Res 2007;86:1198–202.

[12] Xu X, Luo D, Guo C, Rong Q. A custom-made temporomandibular joint prosthesis for fabrication by selective laser melting: Finite element analysis. Med Eng Phys 2017;46:1–11. doi:10.1016/j.medengphy.2017.04.012.

[13] Mesnard M, Ramos A. Towards a rigorous approach to designing a TemporoMandibular joint prosthesis. From clinical challenge to numerical prototype. Procedia CIRP 2013;5:141–6. doi:10.1016/j.procir.2013.01.029.

[14] Hsu JT, Huang HL, Tsai MT, Fuh LJ, Tu MG. Effect of screw fixation on temporomandibular joint condylar prosthesis. J Oral Maxillofac Surg 2011;69:1320–8. doi:10.1016/j.joms.2010.05.074.

[15] Commisso MS, Martínez-Reina J, Ojeda J, Mayo J. Finite element analysis of the human mastication cycle. J Mech Behav Biomed Mater 2015;41:23–35. doi:10.1016/j.jmbbm.2014.09.022.

[16] Kashi A, Chowdhury AR, Saha S. Finite element analysis of a TMJ implant. J Dent Res 2010;89:241–5. doi:10.1177/0022034509357716.

[17] Huang HL, Su KC, Fuh LJ, Chen MYC, Wu J, Tsai MT, et al. Biomechanical analysis of a temporomandibular joint condylar prosthesis during various clenching tasks. J Cranio-Maxillofacial Surg 2015;43:1194–201. doi:10.1016/j.jcms.2015.04.016.

[18] Ackland DC, Moskaljuk A, Hart C, Vee Sin Lee P, Dimitroulis G. Prosthesis Loading After Temporomandibular Joint Replacement Surgery: A Musculoskeletal Modeling Study. J Biomech Eng 2015;137:041001. doi:10.1115/1.4029503.

[19] A. R, M. M. Load transfer in Christensen® TMJ in alloplastic total joint replacement for two different mouth apertures. J Cranio-Maxillofacial Surg 2014;42:1442–9.

[20] Ingawalé S, Goswami T. Temporomandibular joint: Disorders, treatments, and biomechanics. Ann Biomed Eng 2009;37:976–96. doi:10.1007/s10439-009-9659-4.

[21] Sidebottom AJ. Guidelines for the replacement of temporomandibular joints in the United Kingdom. Br J Oral Maxillofac Surg 2008;46:146–7. doi:10.1016/j.bjoms.2006.12.001.

[22] P. M. Relief of pain from headaches and TMJ. Solomon Bookds 1989:1–49.

[23] https://www.sagharbordental.com/ 2019.

[24] Dr. András Fulmer, Dr. Ágnes Bán, Dr. Balázs Gaszner, Dr. Balázs Nagy, Dr. Balázs Sándor, Dr. Bálint Molnár, Dr. Bálint Nemes, Dr. Beáta Benke, Dr. Beáta Kerémi, Dr. Dániel Németh, Dr. Dávid Nagy, Dr. Dezső Szombath, Dr. Dorottya Frank, Dr. Dóra Ottóffy-K U of PD of D and MS. Digital method and content development of the hungarian higher education in dentistry in Hungarian, German and English. Nordex Ltd.; 2014.

[25] K.S. Saladin. Human Anatomy. McGraw-Hill; 2005.

[26] Onoriobe U, Miloro M, Sukotjo C, Mercuri LG, Lotesto A, Eke R. How Many Temporomandibular Joint Total Joint Alloplastic Implants Will Be Placed in the United States in 2030? J Oral Maxillofac Surg 2016;74:1531–8. doi:10.1016/j.joms.2016.04.011.

[27] Mesnard M, Ramos A. Experimental and numerical predictions of Biomet® alloplastic implant in a cadaveric mandibular ramus. J Cranio-Maxillofacial Surg 2016;44:608–15. doi:10.1016/j.jcms.2016.02.004.

[28] Koolstra JH, Van Eijden TMGJ. Combined finite-element and rigid-body analysis of human jaw joint dynamics. J Biomech 2005;38:2431–9. doi:10.1016/j.jbiomech.2004.10.014.

[29] Gonzalez-Perez-Somarriba B, Centeno G, Vallellano C, Gonzalez-Perez LM. On the Analysis of the Contact Conditions in Temporomandibular Joint Prostheses. Adv Mater Sci Eng 2018;2018:1–10. doi:10.1155/2018/2687864.

[30] Ulrich D, Van Rietbergen B, Weinans H, Rüegsegger P. Finite element analysis of trabecular bone structure: A comparison of image-based meshing techniques. J Biomech 1998;31:1187–92. doi:10.1016/S0021-9290(98)00118-3.

[31] Tarala M, Waanders D, Biemond JE, Hannink G, Janssen D, Buma P, et al. The effect of bone ingrowth depth on the tensile and shear strength of the implant-bone e-beam produced interface. J Mater Sci Mater Med 2011;22:2339–46. doi:10.1007/s10856-011-4419-z.

[32] Iguchi H, Magara J, Nakamura Y, Tsujimura T, Ito K, Inoue M. Changes in jaw muscle activity and the physical properties of foods with different textures during chewing behaviors. Physiol Behav 2015;152:217–24. doi:10.1016/j.physbeh.2015.10.004.

[33] Throckmorton GS. Quantitative calculations of temporomandibular joint reaction forces—II. The importance of the direction of the jaw muscle forces. J Biomech 2004;18:453–61. doi:10.1016/0021-9290(85)90280-5.

[34] Korioth, Tom W.P.; Hannam AG. Mandibular Forces During Simulated Tooth Clenching. J Orofac Pain 1994;8:178–89.

[35] Kawakami S, Kodama N, Maeda N, Sakamoto S, Oki K, Yanagi Y, et al. Mechanomyographic activity in the human lateral pterygoid muscle during mandibular movement. J Neurosci Methods 2012;203:157–62. doi:10.1016/j.jneumeth.2011.09.026.

[36] Conci RA, Tomazi FHS, Noritomi PY, Da Silva JVL, Fritscher GG, Heitz C. Comparison of Neck Screw and Conventional Fixation Techniques in Mandibular Condyle Fractures Using 3-Dimensional Finite Element Analysis. J Oral Maxillofac Surg 2015;73:1321–7. doi:10.1016/j.joms.2015.01.037.

[37] www.nf2is.org 2019. https://www.nf2is.org/facial_nerve.php.

[38] Geetha M, Singh AK, Asokamani R, Gogia AK. Ti based biomaterials, the ultimate choice for orthopaedic implants - A review. Prog Mater Sci 2009;54:397–425. doi:10.1016/j.pmatsci.2008.06.004.

[39] Alvarez K, Nakajima H. Metallic scaffolds for bone regeneration. Materials (Basel) 2009;2:790–832. doi:10.3390/ma2030790.

[40] Pancanti A, Bernakiewicz M, Viceconti M. The primary stability of a cementless stem varies between subjects as much as between activities. J Biomech 2003;36:777–85. doi:10.1016/S0021-9290(03)00011-3.

[41] Harrison N, McHugh PE, Curtin W, Mc Donnell P. Micromotion and friction evaluation of a novel surface architecture for improved primary fixation of cementless orthopaedic implants. J Mech Behav Biomed Mater 2013;21:37–46. doi:10.1016/j.jmbbm.2013.01.017.

[42] Mesnard M, Ramos A, Simões JA. Influences of implant condyle geometry on bone and screw strains in a temporomandibular implant. J Cranio-Maxillofacial Surg 2014;42:194–200. doi:10.1016/j.jcms.2013.04.010.

[43] Kienapfel H, Sprey C, Wilke A, Griss P. Implant fixation by bone ingrowth. J Arthroplasty 1999;14:355–68. doi:10.1016/S0883-5403(99)90063-3.

[44] Morra EA, Greenwald AS. Polymer insert stress in total knee designs during high-flexion activities: A finite element study. J Bone Jt Surg - Ser A 2005;87:120–4. doi:10.2106/00004623-200511002-00014.

[45] R.A. P, T.R. T, R.D. C. Failure analysis of a ceramic bearing acetabular component. J Bone Jt Surg - Ser A 2007;89:367–75.

[46] Ramos A, Duarte RJ, Mesnard M. Prediction at long-term condyle screw fixation of temporomandibular joint implant: A numerical study. J Cranio-Maxillofacial Surg 2015;43:469–74. doi:10.1016/j.jcms.2015.02.013.

[47] Brach del Prever EM, Bistolfi A, Bracco P, Costa L. UHMWPE for arthroplasty: Past or future? J Orthop Traumatol 2009;10:1–8. doi:10.1007/s10195-008-0038-y.

[48] Ramos A, Mesnard M. Christensen vs Biomet Microfixation alloplastic TMJ implant: Are there improvements? A numerical study. J Cranio-Maxillofacial Surg 2015;43:1398–403. doi:10.1016/j.jcms.2015.07.009.

[49] Perez DE, Wolford LM, Schneiderman E, Movahed R, Bourland C, Gutierrez EP. Does Unilateral Temporomandibular Total Joint Reconstruction Result in Contralateral Joint Pain and Dysfunction? J Oral Maxillofac Surg 2016;74:1539–47. doi:10.1016/j.joms.2016.02.009.

[50] Wiskott HWA, Botsis J, Scherrer SS, Belser UC. J.1600-0501.2004.01000.X 2004:1–10.

Master's Thesis file

Students: David Pastor Alonso

Title: *Biomechanische evaluatie van een patiënt-specifieke TMJ prothese met behulp van eindige elementen methodes*

English title: Biomechanical evaluation of a patient-specific TMJ prosthesis using FEM

UDC: *612.76*

Content in brief: (maximum 500 words)

The purpose of this study is to evaluate the influence of the patient-specific TMJ prosthesis on the prosthesis components, mandibular bone, opposite joint, and mastication cycle. A finite element model was developed using the state-of-the art techniques to model the relevant anatomical components encountered in the TMJ and the prosthesis. The contacts were modelled according to the equations of contact mechanics, the whole FE model was subjected to a convergence test, and the results were compared to the literature in order to ensure the reliability of the results. Furthermore, several tooth clenching situations were simulated to evaluate the performance of the prosthesis through commonly used parameters (e.g. maximum Von Mises stress/strain). To assess the influence of the TMJR on the remaining healthy tissue, a different FE model of a healthy patient was developed for comparison. Moreover, the implant is equipped with a scaffold that promotes osseointegration. The influence and feasibility of bone ingrowth into the scaffold was also analysed.
Additionally, 4D CT data of the mastication cycle of the patient was used to develop a dynamic FE model of the mastication cycle. This latter model was used to observe the influence of different mandible positions on the stress in both the healthy and prosthetic joint.
The models and techniques used in this study can serve as a first step to the development of a comprehensive FE model that, with some added effort, may be considered as a virtual patient for the TMJ prostheses developed by CADskills.

(Title of the article: Biomechanical Evaluation of a Patient-Specific Prosthesis Using FEM)

Thesis submitted to obtain the degree of Master in Engineering: Biomedical Engineering
Supervisor(s): Prof. Dr. Ir. Jos Vander Sloten and Prof. Dr. Maurice Mommaerts
Assessors: Prof. Dr. Ir. Harry Van Lenthe and Prof. Dr. Ir. Nele Famaey
Mentor(s): Ir. Stijn Huys